

# Mathematical Analysis of HIV-1 Dynamics in Vivo\*

---

Alan S. Perelson<sup>†</sup>  
Patrick W. Nelson<sup>†</sup>

**Abstract.** Mathematical models have proven valuable in understanding the dynamics of HIV-1 infection in vivo. By comparing these models to data obtained from patients undergoing antiretroviral drug therapy, it has been possible to determine many quantitative features of the interaction between HIV-1, the virus that causes AIDS, and the cells that are infected by the virus. The most dramatic finding has been that even though AIDS is a disease that occurs on a time scale of about 10 years, there are very rapid dynamical processes that occur on time scales of hours to days, as well as slower processes that occur on time scales of weeks to months. We show how dynamical modeling and parameter estimation techniques have uncovered these important features of HIV pathogenesis and impacted the way in which AIDS patients are treated with potent antiretroviral drugs.

**Key words.** AIDS, mathematical modeling, HIV

**AMS subject classifications.** 93A30, 92B05, 92C50, 92D25

**PII.** S0036144598335107

---

**1. Introduction.** Infection by human immunodeficiency virus-type 1 (HIV-1) has many puzzling quantitative features. For example, there is an average lag of nearly 10 years between infection with the virus and the onset of AIDS in adults. The reason for this time lag remains largely unknown, although it seems tied to changes in the number of circulating CD4<sup>+</sup> T cells. The major target of HIV infection is a class of lymphocytes, or white blood cells, known as CD4<sup>+</sup> T cells. These cells secrete growth and differentiation factors that are required by other cell populations in the immune system, and hence these cells are also called “helper T cells.” When the CD4<sup>+</sup> T cell count, which is normally around 1000 mm<sup>-3</sup>, reaches 200 mm<sup>-3</sup> or below in an HIV-infected patient, then that person is classified as having AIDS. Because of the central role of CD4<sup>+</sup> T cells in immune regulation, their depletion has widespread deleterious effects on the functioning of the immune system as a whole and leads to the immunodeficiency that characterizes AIDS.

---

\*Received by the editors February 4, 1998; accepted for publication (in revised form) July 11, 1998; published electronically January 22, 1999. Portions of this work were performed under the auspices of the U.S. Department of Energy. This work was supported by NIH grants RR06555 and AI40387. The U.S. Government retains an irrevocable, nonexclusive, royalty-free license to publish, translate, reproduce, use, or dispose of the published form of the work and to authorize others to do the same for U.S. Government purposes.

<http://www.siam.org/journals/sirev/41-1/33510.html>

<sup>†</sup>Theoretical Biology and Biophysics Group and Center for Nonlinear Studies, Theoretical Division, Los Alamos National Laboratory, Los Alamos, NM 87545 ([asp@receptor.lanl.gov](mailto:asp@receptor.lanl.gov)). Current address for the second author: Institute for Mathematics and Its Applications, University of Minnesota, Minneapolis, MN 55455 ([pnelson@ima.umn.edu](mailto:pnelson@ima.umn.edu)).

The reason for the fall in the T cell count is unknown, as are the processes that determine the rate of fall. T cells are normally replenished in the body, and the infection may affect the source of new T cells or the homeostatic processes that control T cell numbers in the body. Although HIV can kill cells that it productively infects, only a small fraction of CD4<sup>+</sup> T cells ( $10^{-4}$  to  $10^{-5}$ ) are productively infected at any one time. Thus, in addition to direct killing of T cells, HIV may have many indirect effects [2, 43].

Over the past decade, a number of models have been developed to describe the immune system, its interaction with HIV, and the decline in CD4<sup>+</sup> T cells. Both stochastic and deterministic models have been developed. Stochastic models [41, 42, 64] can be used to account for the early events in the disease, when there are few infected cells and a small number of viruses, or situations where the variability among individuals is of interest. One class of stochastic models has looked at the effects of increasing variability among viral strains, as a means of escaping control by the immune system, in the progression to AIDS [44, 45, 46, 48], but this approach has been criticized [63, 68]. Deterministic models, which have been developed by many authors [1, 10, 12, 15, 17, 18, 25, 26, 27, 29, 30, 31, 32, 33, 37, 38, 39, 40, 49, 54, 56, 57, 59, 61, 62, 66], examine the changes in mean cell numbers, and are more applicable to later stages of the process in which population sizes are large. These models typically consider the dynamics of the CD4<sup>+</sup> T cell and virus populations as well as the effects of drug therapy. In some of these models other immune system populations, such as macrophages or CD8<sup>+</sup> cells, have been included. Many of these models, and particularly ones developed before 1995, have tended to focus on explaining the kinetics of T cell decline. Unfortunately, many different models have been able to, more or less, mimic this aspect of HIV infection, and to make progress, additional criteria needed to be developed. The impetus for further modeling came with the development of rapid, sensitive, and accurate methods of measuring the number of virus particles in blood. Each virus particle contains two RNA molecules that can be measured by quantitative polymerase chain reaction (PCR)-based methods. Thus, in addition to mimicking changes in T cell kinetics, current models also need to account for the change in the amount of virus detected in blood and possibly other tissues and bodily fluids. Further, experimental methods have been developed that can measure, albeit with less accuracy than the PCR-based methods, the number of infected cells in a tissue or blood sample [6, 19, 51]. Thus, theories also need to explain the dynamical changes in the number of infected cells.

In this article we review recent developments in which modeling has made a substantial impact on our thinking and understanding of HIV infection. Because of the difficulties of doing experiments in humans, fundamental information has been lacking about the dynamics of HIV infection. For example, because the disease takes 10 years, on average, to develop, many people thought that the components of the disease process would also be slow. This has turned out to be incorrect. As we show, modeling combined with appropriate experiments has revealed that HIV is a dynamic disease encompassing a number of different time scales, running from hours to days to weeks to months. We show how perturbation experiments, combined with mathematical modeling, led to the uncovering of these different time scales and to the recognition that these time scales correspond to important biological processes underlying HIV infection. Further, the analysis of such *in vivo* perturbation experiments has helped elucidate the nature of various reservoirs for the virus and raised for serious discussion the intriguing possibility that prolonged therapy with highly

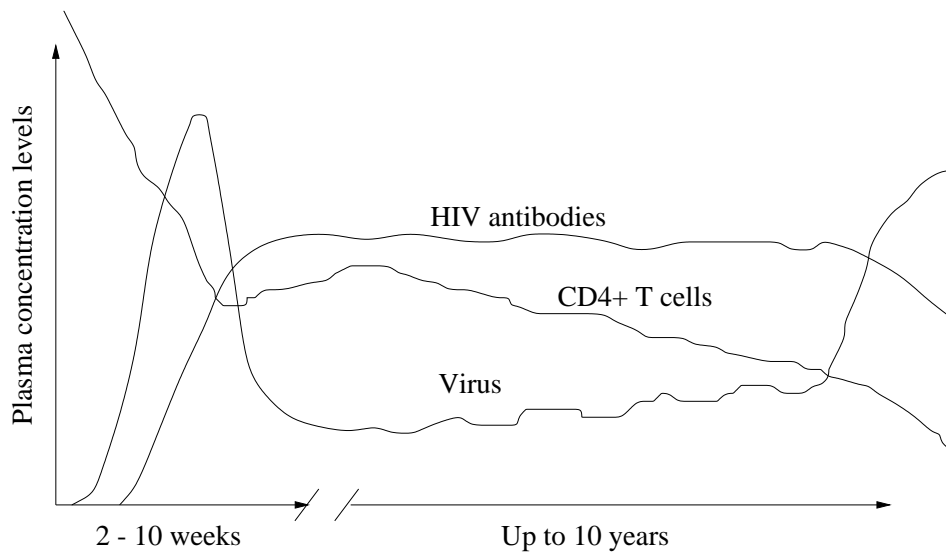


**Fig. 1.1** *Time course of HIV infection in a typical infected adult. The viral load and level of antibodies against HIV are depicted. The early peak in viral load corresponds to primary infection. Primary infection is followed by a long asymptomatic period during which the viral load changes little. Ultimately, the viral load increases and the symptoms of full-blown AIDS appear. On average, the time from infection to AIDS is 10 years, but still some patients progress to AIDS much more rapidly, while others progress more slowly. The graphs here are only meant to be schematic and are not data from any particular patient.*

effective drug combinations might ultimately lead to virus eradication. The fact that HIV replicates rapidly, producing on average  $10^{10}$  viral particles per day, which was uncovered by this approach, led to the realization that HIV was evolving so rapidly that treatment with a single drug was bound to fail. This realization helped speed the recommended form of treatment from monotherapy to combination therapy employing three or more drugs, and has had a major impact in extending people's lives. While virus eradication no longer seems like an easily attainable goal even for patients on combination therapy, modeling still brought home an important practical message: patients should continue taking antiretroviral drugs for a period of at least 2–3 years after virus is no longer detectable in blood. Lastly, mathematical modeling, which at one time was essentially ignored by the experimental AIDS community, has in the last three years become an important tool, and almost all of the major experimental groups are now collaborating with a theorist.

In order to understand the successes of modeling, we begin with an overview of the dynamical features of HIV infection as understood in the early 1990s. The typical course of HIV infection as might have been seen in a textbook [67] or review article is shown in Figure 1.1. Immediately after infection the amount of virus detected in the blood,  $V$ , rises dramatically. Along with this rise in virus, flu-like symptoms tend to appear. After a few weeks to months the symptoms disappear and the virus concentration falls to a lower level. An immune response to the virus occurs and antibodies against the virus can be detected in the blood. A test to detect these antibodies is used to determine if a person has been exposed to HIV. If the antibodies are detected, a person is said to be HIV-positive.

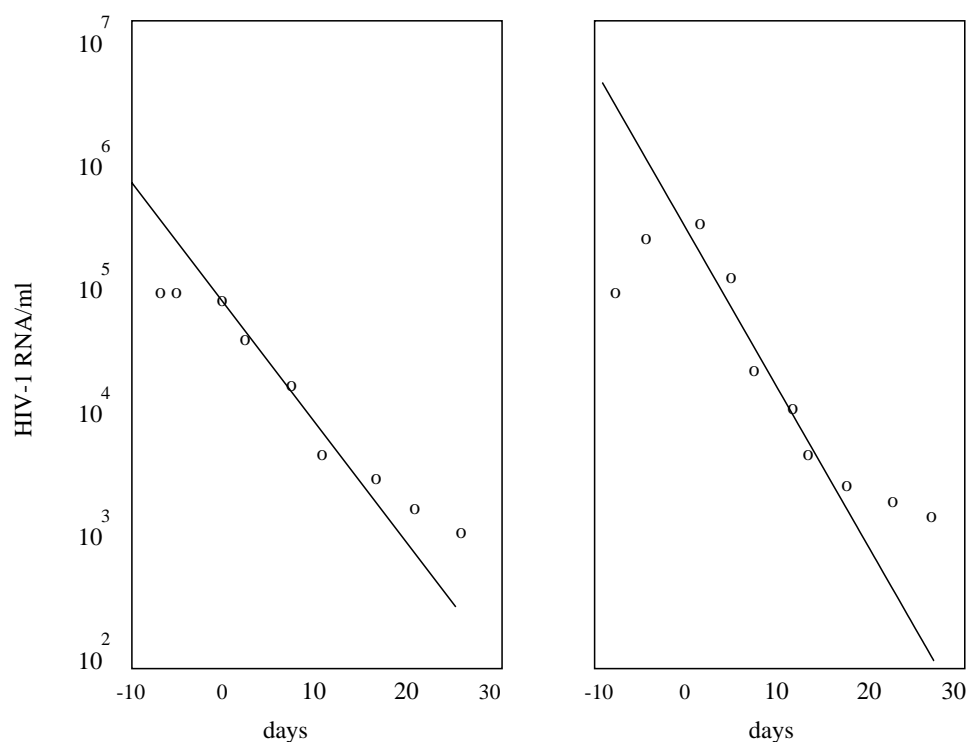


**Fig. 1.2** Plasma viral load before and after treatment with a protease inhibitor, showing rapid decline in viral concentrations after treatment initiation at  $t = 0$ . Each HIV-1 virus particle contains 2 RNA molecules. Data is from 2 out of 20 patients studied in [23]. All 20 patients exhibited similar rapid declines (see Table 2.1).

The level the virus falls to after “primary infection” has been called the set-point. The viral concentration deviates little from this set-point level for many years; however, the concentration of  $CD4^+$  T cells measured in blood slowly declines. This period in which the virus concentration stays relatively constant but in which the T cell count slowly falls is typically a period in which the infected person has no disease symptoms. The asymptomatic period can last as long as 10 years.

The question then arises: What is happening during this asymptomatic period? Many investigators believed that the virus was quiescent or latent during this period, as in other viral diseases such as herpes infection, in which the virus hides out in nerve ganglia and only becomes active for brief periods. One method of determining whether the virus is active is to perturb the host-virus system during the asymptomatic period. Fortunately, means are available for doing so.

In 1994, when the modeling work to be discussed in this review began, potent antiretroviral drugs (the protease inhibitors) were being developed and tested. Giving an antiretroviral drug to a patient is a means of perturbing the system. Working with David D. Ho of the Aaron Diamond AIDS Research Center, we examined the response of 20 patients to a protease inhibitor, zidovudine. The results were dramatic. As shown in Figure 1.2, the amount of virus measured in blood plasma fell rapidly once the drug was given.

**2. The Simplest HIV Dynamic Model.** Although previous modeling work had generated a large number of intricate models of HIV dynamics within individual patients, the data obtained from this perturbation experiment would not support the application of a complicated model. The data appeared to show that the virus concentration fell exponentially for a short period after a patient was placed on a potent antiretroviral drug. Thus, the following model was introduced:

$$(2.1) \quad \frac{dV}{dt} = P - cV,$$

where  $P$  is an unknown function representing the rate of virus production,  $c$  is a constant called the clearance rate constant, and  $V$  is the virus concentration. If the drug completely blocks viral production, i.e., causes  $P = 0$ , then the model predicts that  $V$  will fall exponentially, i.e.,  $V(t) = V_0 e^{-ct}$ , where  $t = 0$  is the time therapy is initiated and  $V(0) = V_0$ . Plotting  $\ln V$  versus  $t$  and using linear regression to determine the slope allowed us to estimate  $c$  and the half-life of virus in the plasma,  $t_{1/2} = \ln 2/c$ .

The notion that virus concentration attains a set-point suggests that before therapy began, the patient was in a quasi-steady state in which  $dV/dt = 0$ . If this were the case, as our data on these patients suggested (see Figure 2.1 for three examples), then by knowing  $c$  and the initial virus concentration  $V_0$ , we could compute the viral production rate before therapy, i.e.,  $P = cV_0$ . Measuring  $V_0$  for each patient, then multiplying this concentration by the fluid volume in which virus is expected to be found, allowed us to compute the total rate of virus production in these patients. These results are summarized in Table 2.1. The rates are minimal estimates because they are based on the hypothesis that the drug completely blocks virus production and hence that the kinetics after drug therapy is initiated is a perfect exponential decline. Although the data appeared to fall exponentially, we knew on theoretical grounds that this could not be the case, because the drug could not instantly block all viral production. Thus, our experiments measured the rate of virus clearance in the face of some residual production, and the slope of the viral decline was not the true clearance rate constant, but only a lower bound. The more refined models given below will illustrate this point. Further, we believe that the viral clearance we measured was a consequence of biological processes in place before the drug was given, since similar rates of decline have been observed with different drugs and with different patient populations (cf. [9, 65]).

**3. A Model that Incorporates Viral Production.** HIV infects cells that carry the CD4 cell surface protein as well as other receptors called coreceptors. Cells that are susceptible to HIV infection are called target cells. The major target of HIV infection is the CD4<sup>+</sup> T cell. After becoming infected, such cells can produce new HIV virus particles, or virions. Thus, to model HIV infection we introduce a population of uninfected target cells,  $T$ , and productively infected cells,  $T^*$ . Later, we shall discuss another state of infection of a cell called latent infection, in which a cell can be infected by the virus but the cell does not produce new virus particles.

The population dynamics of CD4<sup>+</sup> T cells in humans is not well understood. Nevertheless, a reasonable model for this population of cells is

$$(3.1) \quad \frac{dT}{dt} = s + pT \left( 1 - \frac{T}{T_{max}} \right) - d_T T,$$

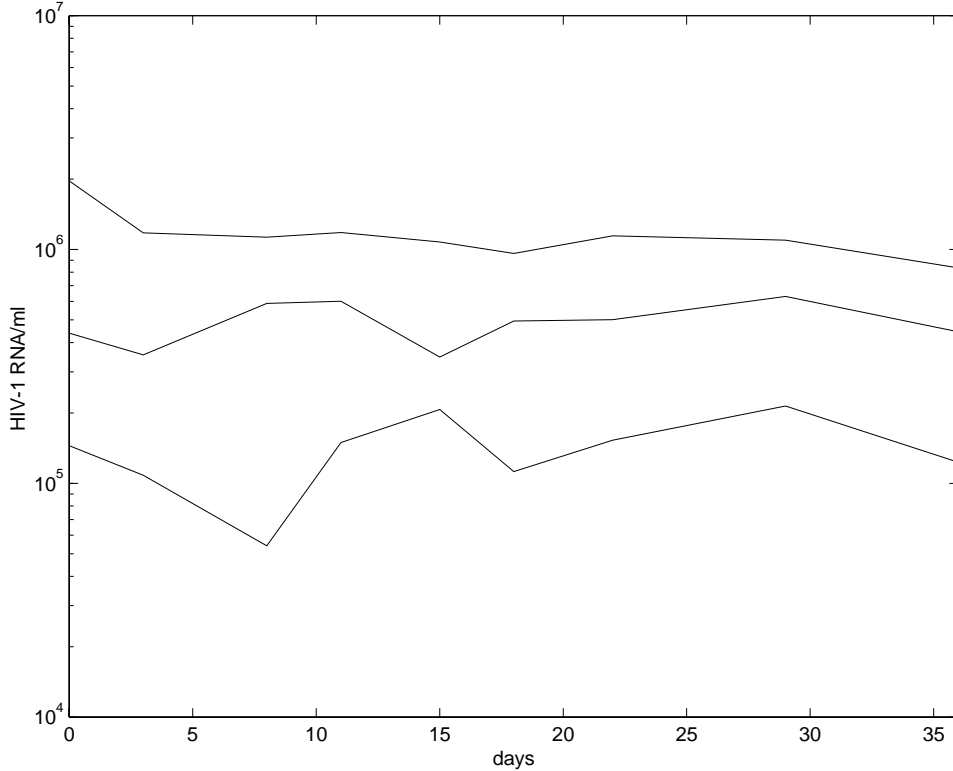


**Fig. 2.1** *The concentration of HIV-1 RNA, measured in plasma, versus time for three patients before initiation of antiretroviral therapy [23].*

where  $s$  represents the rate at which new T cells are created from sources within the body, such as the thymus. T cells can also be created by proliferation of existing T cells. Here we represent the proliferation by a logistic function in which  $p$  is the maximum proliferation rate and  $T_{max}$  is the T cell population density at which proliferation shuts off. While there is no direct evidence that T cell proliferation is described by the logistic equation given above, there are suggestions that the proliferation rate is density-dependent with the rate of proliferation slowing as the T cell count gets high [23, 58]. Lastly, T cells, like all cells, have a natural lifespan. Here  $d_T$  is the death rate per T cell. If the population ever reaches  $T_{max}$  it should decrease; thus we impose the constraint  $d_T T_{max} > s$  [54]. Equation (3.1) has a single stable steady state given by

$$(3.2) \quad \bar{T} = \frac{T_{max}}{2p} \left[ p - d_T + \sqrt{(p - d_T)^2 + \frac{4sp}{T_{max}}} \right],$$

where the overbar denotes a steady state value. In [54], a discussion of biologically realistic choices for the parameters  $p$ ,  $d_T$ ,  $s$ , and  $T_{max}$  is given.

In the presence of HIV, T cells become infected. The simplest and most common method of modeling infection is to augment (3.1) with a “mass-action” term in which the rate of infection is given by  $kVT$ , with  $k$  being the infection rate constant. This type of term is sensible, since virus must meet T cells in order to infect them and

**Table 2.1** Summary of patient CD4 counts, viral load, and deduced HIV-1 kinetics during the pre-treatment quasi-steady state. Adapted from [23]. (A virion is a virus particle.)

Patient	CD4 count ( $\text{mm}^{-3}$ )	Plasma viremia $V_0$ (virions per $\text{ml} \times 10^3$ )	Half-life of virus, $t_{1/2}$ (days)	Minimum production and clearance, $P = cV_0$ (virions/day $\times 10^9$ )
301	76	193	2.3	0.6
302	209	80	2.6	0.3
303	293	41	3.3	0.1
304	174	121	2.5	0.5
305	269	88	2.1	0.5
306	312	175	1.3	1.3
308	386	185	1.5	1.5
309	49	554	2.4	1.9
310	357	15	2.7	0.1
311	107	130	2.4	0.5
312	59	70	2.3	0.3
313	47	100	1.3	0.9
401	228	101	1.7	0.5
402	169	55	2.5	0.2
403	120	126	2.2	0.7
404	46	244	2.6	1.1
406	490	18	2.2	0.1
408	36	23	2.8	0.1
409	67	256	1.5	2.1
410	103	99	1.9	0.5
Range	36 – 490	15 – 554	1.3 – 3.3	0.1 – 2.1
Mean	$180 \pm 46$	$134 \pm 40$	$2.1 \pm 0.4$	$0.7 \pm .1$

the probability of virus encountering a T cell at low concentrations (when  $V$  and  $T$  motions can be regarded as independent) can be assumed to be proportional to the product of their concentrations. Thus, in what follows, we shall assume that infection occurs by virus,  $V$ , interacting with uninfected T cells,  $T$ , causing the loss of uninfected T cells at rate  $-kVT$  and the generation of infected T cells at rate  $kVT$ .

In principle, the rate of infection should saturate at high virus concentration. However, during HIV infection the concentration of virus never gets high compared to the number of T cells. In fact, in the blood of an HIV-1-infected patient a typical ratio might be 1:1 (e.g.,  $10^5$  virions/ml and 100  $\text{CD4}^+$  T cells/ $\mu\text{l}$ ). Similarly, it has been estimated that there are approximately  $10^{11}$  virions and  $10^{11}$   $\text{CD4}^+$  T cells in lymphoid tissue [6]. Thus, we ignore saturation effects. Infection might also occur by cell-to-cell transmission, where an infected cell,  $T^*$ , directly interacts with an uninfected cell,  $T$ . There is little evidence that such direct cell-to-cell infection is a major pathway in vivo, and we shall ignore this mode of infection here.

The models that we focus on are one-compartment models in which  $V$  and  $T$  are identified with the virus concentration and T cell counts measured in blood. Infection is not restricted to blood, and in fact, the vast majority of  $\text{CD4}^+$  T cells are in lymphoid tissue. However, the available data suggests that the concentration of virus and  $\text{CD4}^+$  T cells measured in blood is a reasonable reflection of their concentrations throughout the body (cf. [19, 51]), as one would expect for a system in equilibrium. Clearly transients may develop when this is no longer the case, say, due to an acute infection. Multicompartment models are being developed (cf. [28, 31]) that may eventually provide further insights into disease dynamics.

With the simple mass-action infection term, the rates of change of uninfected cells,  $T$ , productively infected cells,  $T^*$ , and virus,  $V$ , are

$$(3.3) \quad \frac{dT}{dt} = s + pT \left( 1 - \frac{T}{T_{max}} \right) - d_T T - kVT,$$

$$(3.4) \quad \frac{dT^*}{dt} = kVT - \delta T^*,$$

$$(3.5) \quad \frac{dV}{dt} = N\delta T^* - cV.$$

The various terms and parameters are described below.

The probability that an infected (or uninfected) lymphocyte will die as a function of time or cell age is not known. Thus, we have made the simplest possible assumption, that is, that the rate of death per cell is a constant  $d_T$  for uninfected cells and  $\delta$  for infected cells. This is equivalent to the assumption that the probability of cell death at time  $t$  is given by an exponential distribution with an average cell lifetime of  $1/d_T$  for uninfected cells and  $1/\delta$  for infected cells. Other models might incorporate a density-dependent rate of death or use some other intrinsic probability distribution for cell death. For example, one might imagine that the probability of cell death is given by a gamma distribution, which is used to represent multistage processes and can be viewed as suggesting that cell death only occurs after a number of subprocesses are completed. Because distributions like the gamma distribution are specified by two or more parameters, they are not useful at this stage in modeling, where there is no basis for choosing these parameters or any possibility of identifying them from data. Later we will show that from data we can estimate the mean,  $1/\delta$ , of the probability distribution describing cell death.

In the presence of HIV, there are two types of T cells: uninfected and productively infected. Thus, it would be reasonable to change the logistic proliferation term to  $pT(1 - \frac{T+T^*}{T_{max}})$ . However, the proportion of productively infected cells is very small, on the order of  $10^{-4}$  to  $10^{-5}$  of T cells [7], and thus it is sensible to ignore this correction.

Finally, virus is produced by productively infected cells. Here we have assumed that on average each productively infected cell produces  $N$  virions during its lifetime. Since the average lifetime of a productively infected cell is  $1/\delta$ , the average rate of virion production is  $\pi = N\delta$ . In some models it is useful to introduce the parameter  $\pi$ , while for other purposes it is easier to think about (and measure) the total number of virions produced by a cell during its lifetime,  $N$ .

In this equation we have ignored the loss of virus due to infection of a cell. Each time a cell is infected, at least one virion must enter, and thus one might add the term  $-kVT$  to (3.5). In examining the rate of clearance of virions from patients with different T cell counts, we did not find any statistically significant correlation with the T cell count [23]. Thus, it appears as if the term  $kTV$  is small compared to  $cV$  in the average HIV-infected patient. Also, if  $T$  is approximately constant, then one can define a new clearance rate constant,  $c' = c + kT$ , that incorporates loss of virus by infection and other clearance processes. For these reasons we shall not include a  $-kVT$  term in (3.5).

The mechanism of virus clearance from the blood is not known. In fact, binding to cells may be an important part of the clearance mechanism. Thus, one might want to add not only a  $-kVT$  term to equation (3.5) but similar terms for the binding to

other cell populations, e.g., red blood cells, platelets, monocytes, etc. However, as long as these cell populations do not change substantially, they may be considered constants, and hence terms like  $k_1[\text{red blood cell}] + k_2[\text{platelet}] + \dots$  may all be lumped into the constant  $c$ .

**3.1. Analysis.** Before therapy is begun, viral loads are relatively constant. Thus  $dV/dt = 0$ , which implies

$$(3.6) \quad N\delta T_0^* = cV_0,$$

where the subscript 0 is used to denote a pretreatment quasi-steady state value. Because  $V$  is relatively constant for weeks before therapy, this implies that  $T^*$  must also be relatively constant (assuming that the various model parameters  $N$ ,  $c$ , and  $\delta$  are also constant). For  $T^*$  to be constant, we assume  $dT^*/dt = 0$  on this same time scale, and thus

$$(3.7) \quad kV_0T_0 = \delta T_0^*.$$

Generally, the concentration of productively infected cells,  $T^*$ , is not measured in patients. However, T cell counts and viral loads are monitored, and it is reasonable to assume that the  $\text{CD4}^+$  T cell concentration and the viral load are known. The vast majority of cells susceptible to HIV infection are  $\text{CD4}^+$  T cells [52], and we shall assume that  $T_0$  is equal to the  $\text{CD4}^+$  T count at the start of therapy. Using equation (3.7) one can then determine  $T_0^*$ . Thus, for patients in quasi-steady state before antiretroviral therapy begins,  $V_0$ ,  $T_0$ , and  $T_0^*$  provide initial conditions for equations (3.3)–(3.5).

Equations (3.6) and (3.7) imply that for  $V$  and  $T^*$  to be in quasi-steady state,

$$(3.8) \quad NkT_0 = c.$$

This equation will be important in what follows. For example, it implies that patients with different quasi-steady state T cell counts must have differences in one of the parameters  $N$ ,  $k$ , or  $c$ . Further, it suggests that disease progression, characterized by a lowering in the  $\text{CD4}^+$  T cell count, should occur if  $N$  or  $k$  increases with time. Models incorporating these two hypotheses for disease progression have been developed in which it is assumed that within patients, viral evolution drives parameter changes (cf. [11, 50, 54, 59]).

The T cell count changes in HIV-1 infected patients, but on a time scale of years (Figure 1.1). If we assume that on a scale of weeks the T cell count as well as  $V$  and  $T^*$  do not change, then we can compute a full pretreatment steady state. This yields

$$(3.9) \quad T_0 = \frac{c}{Nk}, \quad T_0^* = \frac{cV_0}{N\delta}, \quad \text{and} \quad V_0 = \frac{sN}{c} + \frac{p - d_T}{k} - \frac{pc}{Nk^2T_{max}}.$$

Frequently throughout this paper, we shall examine the situation in which  $T = \text{constant} = T_0$ , but  $T^*$  and  $V$  vary according to equations (3.4) and (3.5), i.e., we analyze the system

$$(3.10) \quad \begin{aligned} \frac{dT^*}{dt} &= kT_0V - \delta T^*, \\ \frac{dV}{dt} &= N\delta T^* - cV. \end{aligned}$$

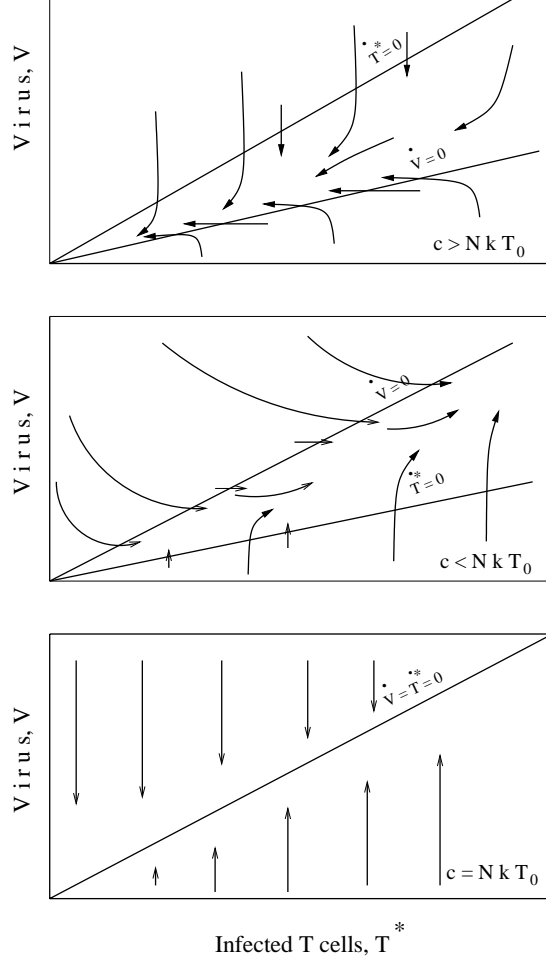


**Fig. 3.1.** Phase portraits for the three different ranges of the virus clearance rate constant  $c$ .

Looking in the phase-plane (Figure 3.1), we see that the equations  $dT^*/dt = 0$  and  $dV/dt = 0$  define the straight lines

$$(3.11) \quad \begin{aligned} V &= \frac{\delta}{kT_0} T^*, \\ V &= \frac{N\delta}{c} T^*, \end{aligned}$$

which either intersect at the origin (Figure 3.1, top two panels) or, if  $c = NkT_0$ , coincide (Figure 3.1, bottom panel).

In the general case, when  $c \neq NkT_0$ , the origin is a stable fixed point if  $c > NkT_0$  and a saddle point when  $c < NkT_0$ . This can be seen from the phase-plane or by computing the eigenvalues about the origin. The characteristic equation is

$$\lambda^2 + (\delta + c)\lambda + \delta(c - NkT_0) = 0,$$

with solutions

$$(3.12) \quad \begin{aligned} \lambda_1 &= -\frac{\delta + c}{2} + \frac{1}{2}\sqrt{(\delta + c)^2 - 4\delta(c - NkT_0)}, \\ \lambda_2 &= -\frac{\delta + c}{2} - \frac{1}{2}\sqrt{(\delta + c)^2 - 4\delta(c - NkT_0)}. \end{aligned}$$

If  $c < NkT_0$ , then  $\lambda_1 > 0$ ,  $\lambda_2 < 0$ , the origin is a saddle point, and the virus will grow without bound. When  $c > NkT_0$ , the eigenvalues are both negative and the virus will ultimately become extinct. Heuristically, the condition  $c > NkT_0$  can be viewed as implying that the rate of clearance of the virus is greater than its rate of production. At the time of initial infection it is reasonable to assume that  $T = \text{constant}$ . Thus, if one is infected with a virus with parameters  $Nk$ , such that  $c > NkT_0$ , this theory predicts that the virus will be eliminated and the infection will not take. Interestingly, when health care workers are stuck by needles contaminated with blood from AIDS patients, the frequency at which such people become HIV positive is very low, maybe 1 in 200 such incidents. Similarly, not every sexual encounter between an HIV-infected person and an uninfected partner results in detectable infection. Both of these observations are consistent with the prediction that not all infections take. However, the ability to clear the virus by a person diagnosed as being infected should not be taken as an established fact. A variety of other experiments have shown that if the virus load ever gets high enough to be reliably measured, i.e., high enough to reliably establish that a person has been infected, then it is extremely unlikely that the virus will ever be cleared spontaneously.

When  $c = NkT_0$ , the two lines in the phase-plane coincide and there exists a line of equilibria with eigenvalues  $\lambda_1 = -(\delta + c)$  and  $\lambda_2 = 0$ ; no single point is stable, but rather the entire line is a set of possible equilibria. If a perturbation drives the system off the line, then the system will return to another equilibrium point on the line. Thus, the state of the system could wander along the line. If  $c$  were not exactly equal to  $NkT_0$  but, say, somewhat smaller, then this wandering would slowly lead to an increase in virus. While the existence of a quasi-steady state value for the viral load is well established, there is still a tendency for the viral load to increase, possibly by a few percent a year. Thus, while  $c = NkT_0$  is the condition for a quasi-steady state, slight variations from this will keep the viral load trajectories between the two lines given by (3.11).

The finding of a manifold of equilibria when  $c = NkT_0$  is noteworthy because it allows for the possibility of the stable maintenance of productively infected cells,  $T^*$ , and virus,  $V$ , at finite positive values. Further, depending on the parameters characteristic of the virus and host, the equilibrium can differ from one patient to the next. This is also true in the more complex three-dimensional system in which the target cell population is allowed to vary. However, because the T cell level in patients generally changes very slowly, substantial insight can be gained from analyzing the simpler two-dimensional system with  $T$  held constant and the parameter constraint  $c = NkT_0$ .

In much of what follows we shall examine the effects of perturbing this two-dimensional system by applying drugs that affect viral replication or viral infectivity. We shall show that analyzing data obtained for a period of one to two weeks following initiation of therapy, so that the assumption  $T = \text{constant} = T_0$  is reasonable, has yielded important insights into the dynamics of HIV infection.

**4. HIV Biology and Drug Therapy.** HIV is an RNA virus. However, when it infects a cell, the enzyme reverse transcriptase (RT), which it carries, makes a DNA copy of its RNA genome. This DNA copy is then integrated into the DNA of the infected cell with the help of another virally encoded enzyme, integrase. The viral DNA, called the “provirus,” is then duplicated with the cell’s DNA every time the cell divides. Thus a cell, once it contains integrated provirus, remains infected for life. The provirus may also remain in the cytoplasm of the cell in unintegrated form. Ultimately this DNA is degraded and thus cells with unintegrated provirus are only transiently infected. A model incorporating transient infection has been developed [15] but will not be discussed here.

Within a T cell the provirus can remain latent, giving no sign of its presence for months or years [24, 16, 69]. Stimulation of the T cell by an antigen or a mitogen can lead to the production of new virus particles that bud from the surface of the infected cell. The budding can take place slowly, sparing the host cell, or it can take place very rapidly, possibly leading to the lysis of the T cell [35].

When new virus particles are produced by an infected cell, the viral DNA is read and viral RNA is made. Some of this RNA is kept as a full-length transcript of the viral DNA and is used as the genetic material packaged into new virus particles. Other RNA copies play the role of messenger RNA and are used as templates for making viral proteins. Without going into detail, many viral proteins, including the enzymes RT, protease, and integrase, are made as one long “polyprotein,” which must then be cleaved by viral protease into single proteins.

Current drug therapies for HIV-infected patients involve inhibiting either RT or HIV protease. If RT is inhibited, HIV can enter a cell but will not successfully infect it; a DNA copy of the viral genome will not be made and the cell will not make viral proteins or virus particles. The viral RNA that enters the cell is not stable and will degrade. If HIV protease is inhibited, cleavage of the viral polyprotein will not occur, and viral particles will be made that lack functional RT, protease, and integrase enzymes. The net effect of blocking HIV protease is that defective or “noninfectious” viral particles are made. The third viral enzyme, integrase, is also a potential target of drug therapy, and a number of pharmaceutical companies are trying to develop integrase inhibitors.

**5. Models of Drug Therapy.** Patients who are in quasi-steady state can be given RT inhibitors, protease inhibitors, or a combination of the two in order to reduce the amount of virus in their bodies. Models have been developed for all three types of therapy.

**5.1. RT Inhibitors.** Our basic model, (3.3)–(3.5), is

$$(5.1) \quad \frac{dT}{dt} = s + pT \left( 1 - \frac{T}{T_{max}} \right) - d_T T - kVT,$$

$$(5.2) \quad \frac{dT^*}{dt} = kVT - \delta T^*,$$

$$(5.3) \quad \frac{dV}{dt} = N\delta T^* - cV.$$

An RT inhibitor blocks infection and hence reduces  $k$ . In the presence of a perfect inhibitor,  $k = 0$  and

$$(5.4) \quad \frac{dT}{dt} = s + pT \left( 1 - \frac{T}{T_{max}} \right) - d_T T,$$

$$(5.5) \quad \frac{dT^*}{dt} = -\delta T^*,$$

$$(5.6) \quad \frac{dV}{dt} = N\delta T^* - cV.$$

The T cell dynamic equations become uncoupled from the viral dynamic equation. Thus, the model predicts that if viral infection has not changed any of the parameters characterizing T cell dynamics, the T cell population should eventually recover and return to its preinfection steady state level.

Productively infected T cells are no longer generated and their number will decay exponentially; i.e.,  $T^*(t) = T_0^* e^{-\delta t}$ . The amount of free virus will also decay but with more complex double exponential behavior,  $V(t) = V_0 e^{-ct} + \frac{N\delta T_0^*}{c-\delta} (e^{-\delta t} - e^{-ct})$ . Assuming quasi-steady state before treatment,  $T_0^* = kV_0 T_0 / \delta$  and  $NkT_0 = c$ , yields

$$(5.7) \quad V(t) = \frac{V_0}{c-\delta} [ce^{-\delta t} - \delta e^{-ct}],$$

a formula presented in [65]. Note that  $c$  and  $\delta$  appear symmetrically in this formula, and thus if measurements of  $V(t)$  are made and compared with this theoretical prediction, the lifetimes of infected cells and free virus cannot be uniquely identified. However, the formula does show that drug therapy should reduce viral load and that the dynamics of virus loss will reflect a combination of viral clearance and loss of productively infected cells.

RT inhibitors, like other drugs, are not perfect. Thus, a more accurate model for the action of an RT inhibitor is

$$(5.8) \quad \frac{dT}{dt} = s + pT \left( 1 - \frac{T}{T_{max}} \right) - d_T T - (1 - \eta_{RT})kVT,$$

$$(5.9) \quad \frac{dT^*}{dt} = (1 - \eta_{RT})kVT - \delta T^*,$$

$$(5.10) \quad \frac{dV}{dt} = N\delta T^* - cV,$$

where  $\eta_{RT}$  is the ‘‘effectiveness’’ of the RT inhibitor. If  $\eta_{RT} = 1$ , the inhibition is 100% effective, whereas if  $\eta_{RT} = 0$ , there is no inhibition. If we assume that for a short period after therapy is initiated,  $T = constant = T_0$ , then equations (5.9) and (5.10) become linear and can be solved. The eigenvalues of this homogeneous linear two-dimensional system are

$$\lambda_{1,2} = -\frac{\delta + c}{2} \pm \frac{1}{2} \sqrt{(\delta + c)^2 - 4\delta[c - (1 - \eta_{RT})NkT_0]}.$$

If we assume the patient was in quasi-steady state before treatment began, then  $NkT_0 = c$  and

$$(5.11) \quad \lambda_{1,2} = -\frac{\delta + c}{2} \pm \frac{1}{2} \sqrt{(\delta + c)^2 - 4\eta_{RT}\delta c}.$$

By letting  $c = \epsilon\delta$ ,  $\epsilon > 0$ , it is easy to show that  $(\delta + c)^2 \geq 4\delta c$ , and hence since  $0 < \eta_{RT} \leq 1$ , the two eigenvalues are real, negative, and distinct. Thus, as  $t \rightarrow \infty$ ,  $T^*$  and  $V$  both approach zero. Hence, if an RT inhibitor is given,  $\eta_{RT} > 0$ , and the only posttreatment steady state is the origin. Moreover, this “uninfected” posttreatment steady state is stable. This conclusion that the virus is eradicated, however, is based on the unrealistic assumption that  $T$  remains constant as  $t \rightarrow \infty$ . In general, one expects that as the virus concentration decreases,  $CD4^+$  T cells will increase in number, as seen in clinical trials [23]. In such circumstances,  $\eta_{RT}$  will need to be larger than some positive critical value in order for the virus to be eliminated [66].

**5.2. Protease Inhibitors.** Protease inhibitors cause infected cells to produce non-infectious virions. Virions that were created prior to drug treatment remain infectious. Thus, in the presence of a protease inhibitor, we consider two types of virus particles: infectious virions at concentration  $V_I$  and noninfectious virions at concentration  $V_{NI}$ . This notation is somewhat imprecise, since even in the absence of a protease inhibitor, not every virus particle is infectious. Thus, to be more precise,  $V_I$  denotes the population of virus particles that have not been influenced by a protease inhibitor and hence had their polyproteins cleaved, whereas  $V_{NI}$  denotes the population of virus particles with uncleaved polyproteins. Further, we let  $V = V_I + V_{NI}$  be the total virus concentration.

After a 100% effective protease inhibitor is given, the equations of our basic model (5.1) become

$$\begin{aligned} \frac{dT}{dt} &= s + pT \left(1 - \frac{T}{T_{max}}\right) - d_T T - kV_I T, \\ \frac{dT^*}{dt} &= kV_I T - \delta T^*, \\ \frac{dV_I}{dt} &= -cV_I, \\ \frac{dV_{NI}}{dt} &= N\delta T^* - cV_{NI}. \end{aligned} \tag{5.12}$$

Before therapy is initiated,  $V_{NI}(0) = 0$  and all virus belongs to the “infectious pool”; i.e.,  $V_I(0) = V_0$ . Thus,  $V_I(t) = V_0 e^{-ct}$ , and as infectious virus decays, the uninfected T cell population,  $T(t)$ , increases, ultimately returning to the steady state it had in the absence of viral infection (again assuming that infection has not caused any of the parameters characterizing the T cell population to change).

Over a short period of time, immediately after therapy is initiated, one can assume that  $T = \text{constant} = T_0$ . Making this assumption and substituting  $V_I(t)$  into the differential equation for  $T^*$ , one obtains a linear equation with solution

$$T^*(t) = T^*(0)e^{-\delta t} + \frac{kT_0V_0(e^{-ct} - e^{-\delta t})}{\delta - c}. \tag{5.13}$$

Assuming  $T^*$  is in quasi-steady state before initiation of therapy,  $T^*(0) = kV_0T_0/\delta$  and (5.13) becomes

$$T^*(t) = kV_0T_0 \left[ \frac{ce^{-\delta t} - \delta e^{-ct}}{\delta(c - \delta)} \right]. \tag{5.14}$$

**Table 5.1** *Summary of HIV-1 clearance rate, infected cell loss rate, and virion production rate for three patients. Baseline values are measured from one week prior to administration of drug.*

Patient number	Baseline value		Pharm. delay (hours)	Virus clearance		Infected cell loss		Total virus production ( $10^9$ /day)
	CD4 cell ( $\text{mm}^{-3}$ )	Plasma virus ( $10^3$ /ml)		$c$ ( $\text{day}^{-1}$ )	$t_{1/2}$ days	$\delta$ ( $\text{day}^{-1}$ )	$t_{1/2}$ days	
102	16	294	2	3.8	0.2	0.3	2.7	12.9
103	408	12	6	2.7	0.3	0.7	1.0	0.4
104	2	52	2	3.7	0.2	0.5	1.4	2.9
105	11	643	6	2.1	0.3	0.5	1.3	32.1
107	412	77	2	3.1	0.2	0.5	1.4	3.0
Mean	170	216	3.6	3.1	0.2	0.5	1.6	10.3
$\pm$ SD	196	235	2.0	0.6	0.1	0.1	0.6	11.7

Substituting this value of  $T^*(t)$  into the differential equation for  $V_{NI}$  yields a linear time-varying equation with solution

$$(5.15) \quad V_{NI}(t) = \frac{cV_0}{c - \delta} \left[ \frac{c}{c - \delta} (e^{-\delta t} - e^{-ct}) - \delta t e^{-ct} \right],$$

where we have used the quasi-steady state condition  $NkT_0 = c$ . Finally, the total concentration of virus, which is the easily measured quantity, is given by

$$(5.16) \quad V(t) = V_0 e^{-ct} + \frac{cV_0}{c - \delta} \left[ \frac{c}{c - \delta} (e^{-\delta t} - e^{-ct}) - \delta t e^{-ct} \right].$$

Equation (5.16) has been used to analyze patient data [55]. The protease inhibitor ritonavir was administered orally (1200 mg/day) to five HIV-infected patients, whose baseline CD4 cell counts and viral loads are shown in Table 5.1. HIV-1 RNA levels in plasma were measured after treatment at frequent intervals. Each HIV virus particle contains two RNA molecules, and thus the HIV-1 RNA level is a direct measure of the virus concentration,  $V$ . As shown in Figure 5.1, each patient responded with a similar pattern of viral decay, with an initial lag followed by an approximately exponential decline in plasma viral RNA.

After ritonavir was administered, a delay in its antiviral effect was expected due to the time required for drug absorption, distribution, and penetration into the target cells. This pharmacokinetic delay could be estimated by the time elapsed before the first drop in the titer of infectious HIV-1 in plasma (Table 5.1; Figure 5.2). However, even after the pharmacokinetic delay was accounted for, a lag of  $\simeq 1$  day was observed before the level of plasma viral RNA fell (Figure 5.1). This additional delay is consistent with the mechanism of action of protease inhibitors, which render newly produced virions noninfectious but which inhibit neither the production of virions from already infected cells nor the infection of new cells by previously produced infectious virions. These features of the action of a protease inhibitor are incorporated into our model and produce a “shoulder region” in which there is little initial viral decay.

Using nonlinear regression analysis, we estimated  $c$ , the viral clearance rate constant, and  $\delta$ , the rate of loss of virus-producing cells, for each of the patients by fitting (5.16) to the plasma HIV-1 RNA measurements after an adjustment of  $t = 0$  was made to account for the pharmacological delay (Table 5.1). The curves generated

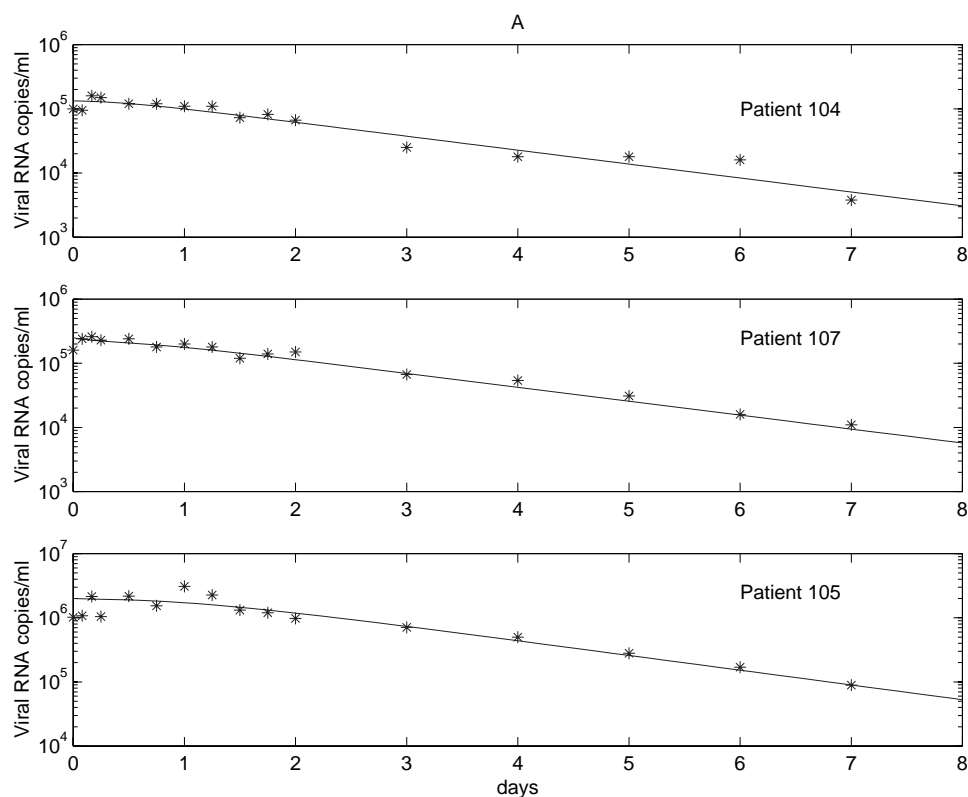


**Fig. 5.1** Data from three patients ( $\star$ ) compared to the model predictions (solid lines). Parameter values corresponding to the best-fit theoretical curves are listed in Table 5.1.

from (5.16), using the best-fit values of  $c$  and  $\delta$ , gave an excellent fit to the data for all patients (Figure 5.1).

Clearance of free virions was the more rapid process, occurring on a time scale of hours. The values of  $c$  ranged from 2.1 to 3.8  $\text{day}^{-1}$  with a mean of  $3.1 \pm 0.6 \text{ day}^{-1}$  (Table 5.1). The corresponding half-life,  $t_{1/2}$ , of free virions ( $t_{1/2} = \ln 2/c$ ) ranged from 0.2 days to 0.3 days with a mean of  $0.24 \pm 0.06$  days ( $\sim 6$  hours). Because data was collected every 2 hours for the first 6 hours and then every 6 hours until day 2, there were not very many data points contributing to the estimate of  $c$ , and large confidence intervals resulted [55]. In order to confirm that viral clearance was as rapid as predicted by this model, an additional experiment was done in which the concentration of infectious virions in plasma,  $V_I$ , was measured in the one patient with the highest initial viral load. Theory predicted that  $V_I(t) = V_0 e^{-ct}$ . For this patient, as shown in Figure 5.2, the infectivity of the patient's plasma when plotted on a logarithmic scale fell linearly with time, and the slope of the curve corresponded to an estimated  $t_{1/2} = 0.23$  days, thus confirming the estimate of  $c$ .

The loss of virus-producing cells, as estimated from the fit of (5.16) to the HIV-1 RNA data, was slower than that of free virions, with values of  $\delta$  ranging from 0.3 to 0.7  $\text{day}^{-1}$ , and a mean of  $0.5 \pm 0.1 \text{ day}^{-1}$ , corresponding to  $t_{1/2}$  values between 1.0 and 2.7 days, with a mean of  $1.6 \pm 0.6$  days (Table 5.1). Note that the lifespans of productively infected cells,  $1/\delta$ , were not dramatically different among the study subjects, even

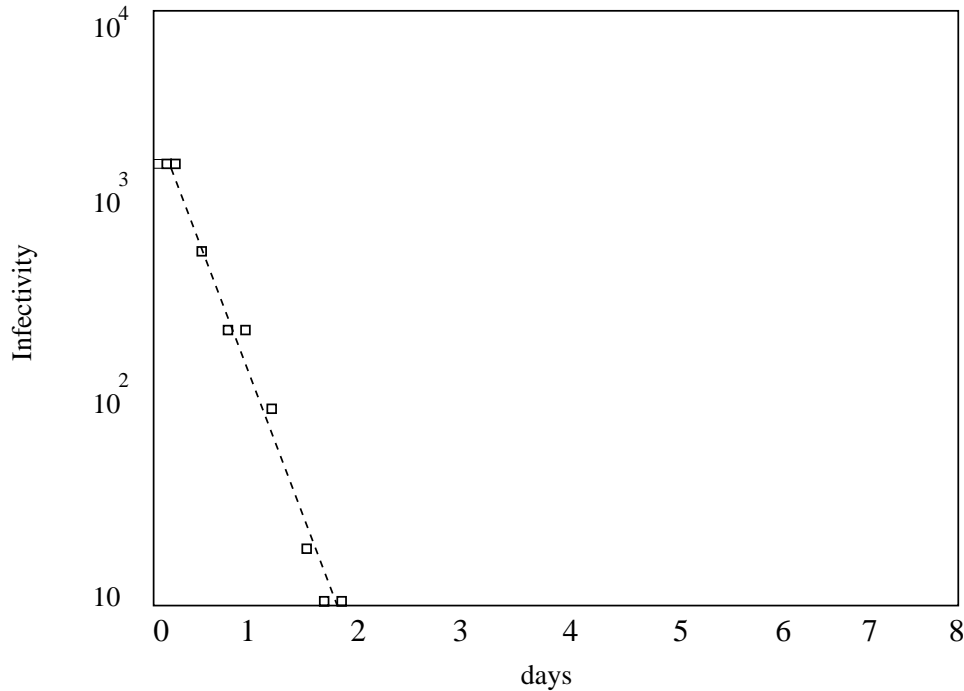


**Fig. 5.2** Best fit of the equation for  $V_I(t)$  to plasma infectivity data obtained from patient 105. The infectivity of the plasma is proportional to the number of infectious virions it contains. See [55] for further experimental details.

though patients with low CD4 lymphocyte counts generally had decreased numbers of virus-specific cytotoxic T cells that in principle can kill productively infected T cells [5].

**5.3. Viral Production.** At steady state, the production rate of virus must equal its clearance rate,  $cV_0$ . Using the estimate of  $c$  and the pretreatment viral level,  $V_0$ , we can obtain an estimate for the rate of viral production before protease inhibitor administration. The product  $cV_0$  gives the number of virions produced per ml of plasma per day. To compute the total number of virions produced per day we multiply  $cV_0$  by the total fluid volume that virions are expected to be suspended in. A typical 70 kg man has a fluid volume of about 15 liters. Table 5.1 gives an estimate of each patient’s viral production based on a calculation of plasma and extracellular fluid volumes using the patient’s body weight. The total daily viral production and clearance rates ranged from  $0.4 \times 10^9$  to  $32.1 \times 10^9$  virions per day, with a mean of  $10.3 \times 10^9$  virions per day released into the extracellular fluid (Table 5.1). These estimates are still minimal estimates, since they are based on the assumption that ritonavir totally blocked all infectious virus production. Additional infection and viral production is probably occurring, and thus the true viral clearance rate is expected to be higher than our estimate. Further, not all virus that is produced is in extracellular fluid, and the estimate does not take this into account.

**5.4. Imperfect Protease Inhibition.** Protease inhibitors are not perfect drugs. Let  $\eta_{PI}$  be the effectiveness of a protease inhibitor or combination of protease in-

inhibitors in blocking production of infectious virions. Then (5.12) can be modified to the form,

$$\begin{aligned}
\frac{dT}{dt} &= s + pT \left(1 - \frac{T}{T_{max}}\right) - d_T T - kV_I T, \\
\frac{dT^*}{dt} &= kV_I T - \delta T^*, \\
\frac{dV_I}{dt} &= (1 - \eta_{PI}) N \delta T^* - cV_I, \\
\frac{dV_{NI}}{dt} &= \eta_{PI} N \delta T^* - cV_{NI}.
\end{aligned}
\tag{5.17}$$

We analyze this model when  $T = \text{constant} = T_0$ . We first solve the two-dimensional linear subsystem for  $T^*$  and  $V_I$ . Assuming a pretreatment steady state, so that  $c = NkT_0$ , we obtain

$$\begin{aligned}
T^*(t) &= \frac{V_0 k T_0}{\lambda_2 - \lambda_1} \left[ \frac{\lambda_2 + c\eta_{PI}}{\lambda_1 + \delta} e^{\lambda_1 t} - \frac{\lambda_1 + c\eta_{PI}}{\lambda_2 + \delta} e^{\lambda_2 t} \right], \\
V_I(t) &= \frac{V_0}{\lambda_2 - \lambda_1} [(\lambda_2 + c\eta_{PI})e^{\lambda_1 t} - (\lambda_1 + c\eta_{PI})e^{\lambda_2 t}],
\end{aligned}
\tag{5.18}$$

where

$$\lambda_{1,2} = -\frac{c + \delta}{2} \pm \frac{1}{2} \sqrt{(c + \delta)^2 - 4\eta_{PI}\delta c}.
\tag{5.19}$$

These eigenvalues are identical in form to those derived for the RT inhibitor model in section 5.1. Thus, the eigenvalues are real, distinct, and negative.

Substituting these solutions for  $T^*$  and  $V_I$  into the differential equation for  $V_{NI}$  and solving, one finds

$$\begin{aligned}
V_{NI}(t) &= \frac{N\eta_{PI}\delta k T_0 V_0}{\lambda_2 - \lambda_1} \left[ \frac{\lambda_2 + c\eta_{PI}}{(\lambda_1 + \delta)(\lambda_1 + c)} e^{\lambda_1 t} - \frac{\lambda_1 + c\eta_{PI}}{(\lambda_2 + \delta)(\lambda_2 + c)} e^{\lambda_2 t} \right. \\
&\quad \left. - \left( \frac{\lambda_2 + c\eta_{PI}}{(\lambda_1 + \delta)(\lambda_1 + c)} + \frac{\lambda_1 + c\eta_{PI}}{(\lambda_2 + \delta)(\lambda_2 + c)} \right) e^{-ct} \right].
\end{aligned}$$

This equation can be simplified by noticing that according to the characteristic equation for the two-dimensional  $T^*$  and  $V$  subsystem,

$$\lambda^2 + (c + \delta)\lambda + \eta_{PI}\delta c = 0,$$

or

$$c\delta = \frac{(\lambda_i + \delta)(\lambda_i + c)}{1 - \eta_{PI}}, \quad i = 1, 2.$$

Thus,

$$V_{NI}(t) = \frac{V_0 \eta_{PI}}{(1 - \eta_{PI})} \left[ \frac{(\lambda_2 + c\eta_{PI})e^{\lambda_1 t} - (\lambda_1 + c\eta_{PI})e^{\lambda_2 t}}{(\lambda_2 - \lambda_1)} - e^{-ct} \right].
\tag{5.20}$$

Adding  $V_I$  and  $V_{NI}$  gives the total virus

$$(5.21) \quad V(t) = \frac{V_0}{(1 - \eta_{PI})} \left[ \frac{(\lambda_2 + c\eta_{PI})e^{\lambda_1 t} - (\lambda_1 + c\eta_{PI})e^{\lambda_2 t}}{(\lambda_2 - \lambda_1)} - \eta_{PI}e^{-ct} \right].$$

If the drug effectiveness  $\eta_{PI}$  is close to 1, then the  $1 - \eta_{PI}$  term in the denominator can cause difficulties in numerical work. This singularity can be avoided by using the characteristic equation and the steady state condition  $NkT_0 = c$  to replace  $1 - \eta_{PI}$  with  $(\lambda_1 + c)(\lambda_1 + \delta)/\delta c$ .

While this solution is more complex than that given by (5.16), it reduces to the simpler form when  $\eta_{PI} = 1$ . This can be seen by using the substitution for  $1 - \eta_{PI}$  given above coupled with l'Hôpital's rule, and noting that when  $\eta_{PI} = 1$ ,  $\lambda_1 = -\delta$  and  $\lambda_2 = -c$ .

**5.4.1. Patients Not in Quasi-Steady State.** It is not necessary to assume that patients are in quasi-steady state prior to treatment initiation, hence  $c \neq NkT_0$ . This assumption gives a more general characteristic equation with eigenvalues,

$$\lambda_{1,2} = -\frac{\delta + c}{2} \pm \frac{1}{2} \sqrt{(\delta - c)^2 + 4(1 - \eta_{PI})NkT_0\delta}.$$

Notice that these eigenvalues differ from (5.19) and provide a means for studying the model's predictions for cases when patients are not at a steady state when treatment is initiated.

A bifurcation occurs at

$$c = NkT_0(1 - \eta_{PI}),$$

or equivalently at

$$\eta_{PI} = 1 - \frac{c}{NkT_0}.$$

If  $\eta_{PI} > 1 - \frac{c}{NkT_0}$ , then both eigenvalues are negative and the virus is predicted to be cleared from the plasma. If  $\eta_{PI} < 1 - \frac{c}{NkT_0}$ , then therapy will not be effective and the virus will continue to grow. Notice that if  $\eta_{PI} = 1$ , then, as we have already shown, the stability analysis predicts the virus will always be eliminated since the eigenvalues become  $\lambda_1 = -c, \lambda_2 = -\delta, \lambda_3 = -c$ . For  $\eta_{PI} = 1$  the solution (5.16) contains a secular term, which for small enough values of  $c$  allows for a growth in the viral population before decaying to zero. The decay of  $V(t)$  is monotonic if  $c \geq NkT_0$  and when  $c < NkT_0$ , the virus is increasing when therapy is initiated, and will continue to increase for a while under therapy, as illustrated in Figure 5.3.

**5.4.2. Decay Slope Is Proportional to Drug Effectiveness: Approximation to Largest Eigenvalue.** Figure 5.4 shows how the rate of viral decay depends upon the effectiveness of the protease inhibitor. Clearly, the higher the effectiveness of the drug the faster the viral decay. To be more precise, we rewrite the largest eigenvalue from (5.19) as

$$\lambda_1 = -\frac{c + \delta}{2} + \frac{c + \delta}{2} \sqrt{1 - \frac{4\delta c\eta_{PI}}{(\delta + c)^2}}.$$

The parameter estimates in Table 5.1 show that  $c \gg \delta$ , so that we can expand the square root to obtain

$$\lambda_1 \sim -\frac{c + \delta}{2} + \frac{c + \delta}{2} \left( 1 - \frac{2\delta c\eta_{PI}}{(c + \delta)^2} + \dots \right),$$

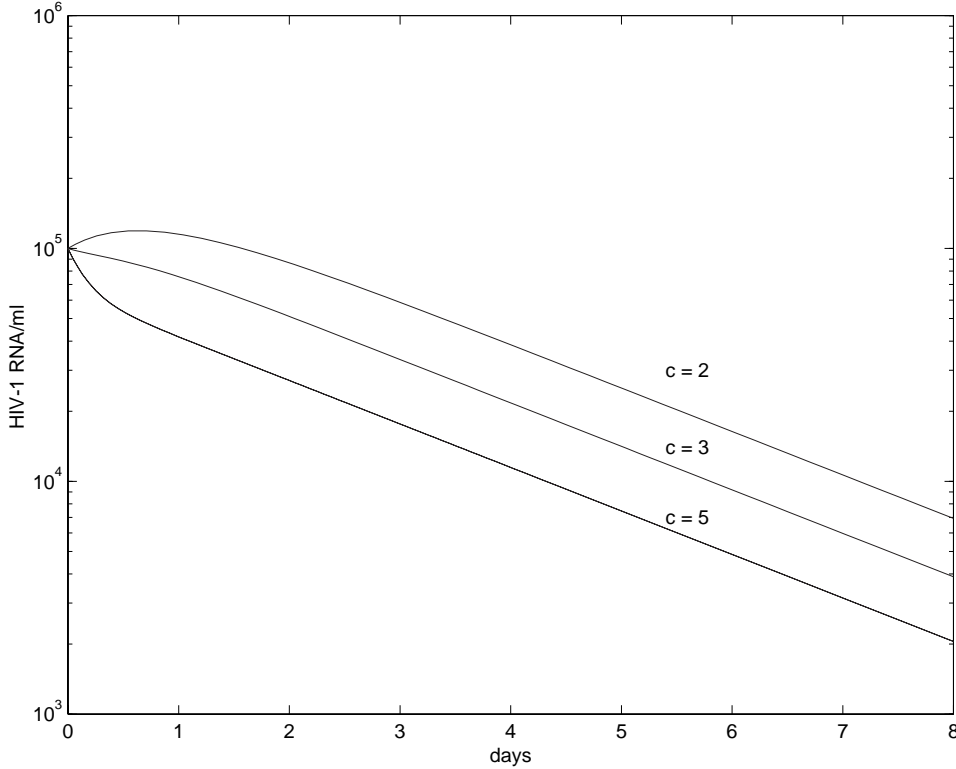


**Fig. 5.3** Prediction of viral decay under 100% effective protease inhibition ( $\eta_{PI} = 1$ ) when the assumption of a pretreatment steady state is not made. Here  $NkT_0 = 2.56 \text{ day}^{-1}$ , and the viral load  $V$  initially increases if the clearance rate  $c$  is less than this value.

and obtain  $\lambda_1 \sim -\delta c \eta_{PI} / (c + \delta) \sim -\delta \eta_{PI}$ . Thus, to first order, the initial slope of viral decay after therapy initiation depends on the product of the death rate of productively infected cells,  $\delta$ , and the effectiveness of the therapy,  $\eta_{PI}$ . This is an important result and it can be used to compare the effectiveness of different doses of protease inhibitors [14].

**5.5. The Effects of T Cell Recovery on Viral Dynamics.** In the previous analyses we have assumed that  $T = \text{constant} = T_0$ . However, after antiretroviral therapy is initiated, some recovery of T cells is observed. Data obtained in [23] suggests that over a period of weeks the recovery of T cells can be described by either a linear or exponential function of time, with no statistically significant difference between the two functions. Recall that we have suggested that T cell dynamics can be summarized by the equation

$$\frac{dT}{dt} = s + pT \left( 1 - \frac{T}{T_{max}} \right) - d_T T - kV_I T.$$

After therapy is initiated  $V_I(t)$  falls rapidly (for a perfect protease inhibitor,  $V_I(t) = V_0 e^{-ct}$ ), and thus after a few days the term  $-kV_I T$  should be negligible. T cell replacement can be due to the source  $s$ , which incorporates the generation of new cells in the thymus and their export into the blood and the transport of already

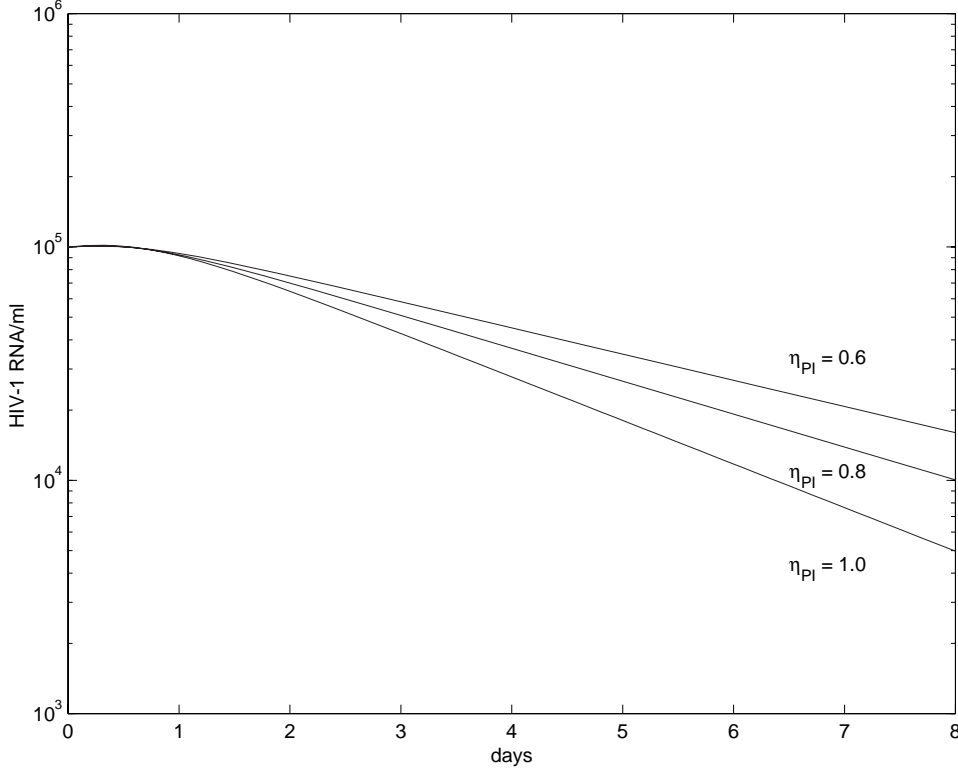


**Fig. 5.4** Plot showing the viral decay for different efficacies of the protease inhibitor from (5.21). As predicted in section 5.4.2, the slope of the viral decay curve is proportional to the effectiveness of the protease inhibitor,  $\eta_{PI}$ .

created T cells in tissues to the blood, or to proliferation of cells. If the source is the major mechanism of T cell replacement, then we can approximate the T cell dynamics by

$$\frac{dT}{dt} = s - d_T T$$

or

$$(5.22) \quad T(t) = T_0 + \alpha t,$$

where  $\alpha = s/d_T$ . Patient data exhibiting a linear increase in CD4<sup>+</sup> T cells is shown in Figure 5.5.

We will first study this linear model and then a nonlinear model that incorporates proliferation.

For  $T(t)$  given by (5.22), the model is

$$(5.23) \quad \frac{dT^*}{dt} = kV_I(\alpha t + T_0) - \delta T^*,$$

$$(5.24) \quad \frac{dV_I}{dt} = (1 - \eta_{PI})N\delta T^* - cV_I,$$

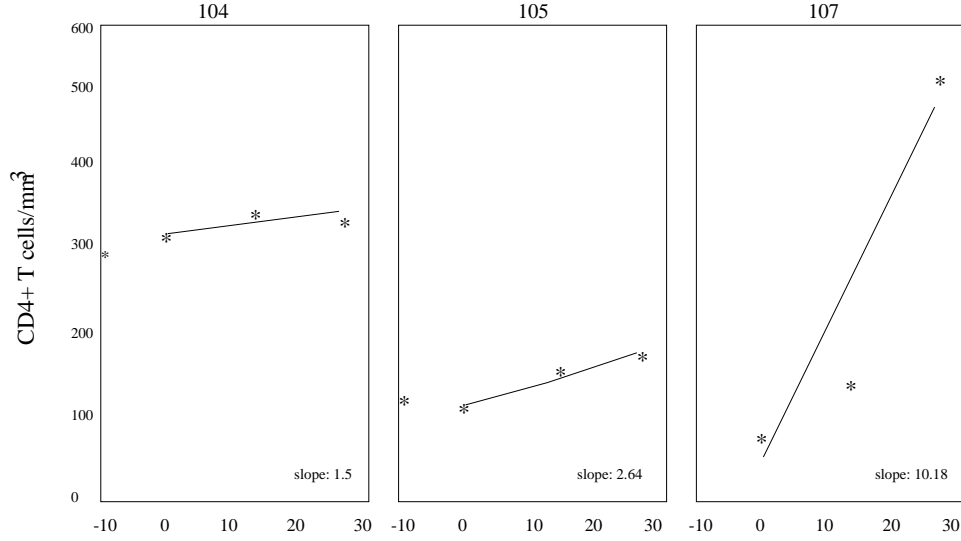


**Fig. 5.5** Increase in  $CD4^+$  T cells after treatment with a protease inhibitor. Data is for three different patients studied in [23].

$$(5.25) \quad \frac{dV_{NI}}{dt} = \eta_{PI} N \delta T^* - cV_{NI}.$$

Rewriting equations (5.23) and (5.24) as a second-order equation in  $V_I$  gives

$$\frac{d^2 V_I}{dt^2} + (c + \delta) \frac{dV_I}{dt} + [\delta c - (1 - \eta_{PI}) N k \delta (\alpha t + T_0)] V_I = 0.$$

The substitution  $V_I(t) = e^{-\frac{(c+\delta)t}{2}} Y(t)$  yields

$$Y'' + \zeta(t) Y = 0,$$

where

$$\zeta(t) = -\frac{(c + \delta)^2}{4} + (\delta c - (1 - \eta_{PI}) N k (\alpha t + T_0) \delta).$$

We can rewrite  $\zeta(t)$  as  $\zeta(t) = a + bt$  with  $a$  and  $b$  constants, and define a transformation of the independent variable as  $s = a + bt$ , to get

$$Y_{ss} - b^2 s Y = 0,$$

which is an Airy equation for which analytical solutions are known. Hence, using the initial conditions and numerical evaluation methods, we have an explicit solution to compare with experimental data. Figure 5.6 shows the solution and its fit with experimental data from three patients. Interestingly, explicitly taking the change in  $CD4^+$  T cells that occurs over the course of one week of therapy into account has little effect on the overall change in HIV-1 RNA.

Now consider the case where  $T$  is varying nonlinearly due to both a source and proliferation. The equations we study are given by (5.17). Because the equations are

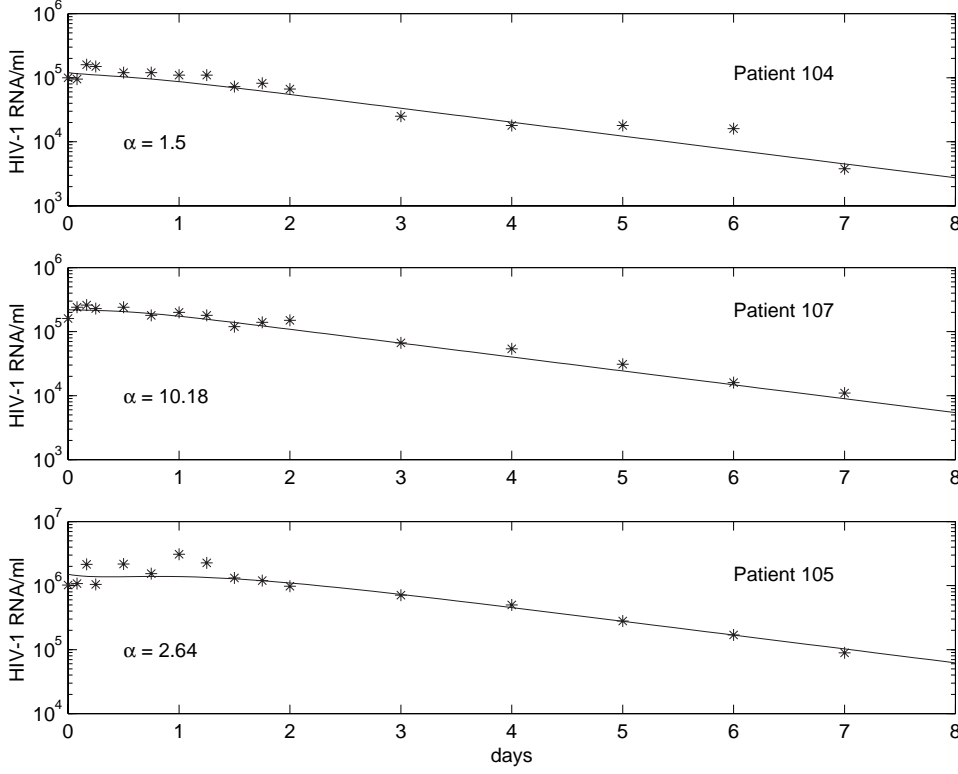


**Fig. 5.6** The effect of a linear increase in  $T$  on viral dynamics. Graph showing model predictions plotted with patient data. The values for  $\alpha$  were determined by linear regression analysis of the change in  $CD4^+$   $T$  cell levels for each patient after drug treatment (Figure 5.5). The plotted curves are indistinguishable from the theoretical curves shown in Figure 5.1, generated assuming  $T = \text{constant} = T_0$ .

nonlinear we cannot solve them explicitly. However, we note that the solution trajectories remain in the positive quadrant for all time since  $\frac{dT}{dt}|_{T=0} = s > 0$ ,  $\frac{dT^*}{dt}|_{T^*=0} = kV_I T > 0$ ,  $\frac{dV_I}{dt}|_{V_I=0} = (1 - \eta_{PI})N\delta T^* > 0$ ,  $\frac{dV_{NI}}{dt}|_{V_{NI}=0} = \eta_{PI}N\delta T^* > 0$ .

We next investigate the steady states of (5.17) and their stability.

**5.5.1. The Steady States.** There are two steady states, which we call noninfected and infected. The *noninfected steady state* has no virus or infected cells present and hence is  $(T_{ss1}, 0, 0, 0)$ , where

$$(5.26) \quad T_{ss1} = \frac{T_{max}}{2p} \left[ p - d_T + \sqrt{(p - d_T)^2 + \frac{4sp}{T_{max}}} \right].$$

The *infected steady state* is

$$T_{ss2} = \frac{c}{Nk(1 - \eta_{PI})}, \quad \bar{V}_I = \frac{s}{kT_{ss2}} + \frac{p(1 - \frac{T_{ss2}}{T_{max}}) - d_T}{k},$$

$$\bar{T}^* = \frac{c\bar{V}_I}{\delta N(1 - \eta_{PI})}, \quad \bar{V}_{NI} = \frac{\eta_{PI}\bar{V}_I}{1 - \eta_{PI}},$$

where overbars again denote steady state quantities. In the absence of treatment,  $\eta_{PI} = 0$ , and under this condition  $T_{ss2}$  reduces to the full pretreatment steady state discussed in section 3. However, here we are interested in the steady state that obtains under treatment, i.e., with  $\eta_{PI} \neq 0$ .

**5.5.2. Stability of the Noninfected Steady State.** The Jacobian matrix evaluated at this steady state is

$$\begin{pmatrix} p\left(1 - \frac{2T_{ss1}}{T_{max}}\right) - d_T & 0 & -kT_{ss1} & 0 \\ 0 & -\delta & kT_{ss1} & 0 \\ 0 & \delta N(1 - \eta_{PI}) & -c & 0 \\ 0 & \delta N\eta_{PI} & 0 & -c \end{pmatrix},$$

with eigenvalues

$$\begin{aligned} \lambda_1 &= p\left(1 - \frac{2T_{ss1}}{T_{max}}\right) - d_T, \\ \lambda_{2,3} &= -\frac{c + \delta}{2} \pm \frac{1}{2}\sqrt{(c + \delta)^2 - 4c\delta + 4\delta NkT_{ss1}(1 - \eta_{PI})}, \\ \lambda_4 &= -c. \end{aligned}$$

For stability we require  $\lambda_1 < 0$  or  $T_{ss1} > \frac{(p-d_T)T_{max}}{2p}$ , a condition that is obviously satisfied (see (5.26)). The eigenvalue with the negative square root term,  $\lambda_3 < 0$ . Lastly, for stability we require  $\lambda_2 < 0$ , which is satisfied if

$$c + \delta > \sqrt{(c + \delta)^2 - 4c\delta + 4\delta NkT_{ss1}(1 - \eta_{PI})}.$$

Hence for stability,

$$c > NkT_{ss1}(1 - \eta_{PI}),$$

or

$$\eta_{PI} > 1 - \frac{c}{NkT_{ss1}}.$$

Thus, as one might expect, if the protease inhibitor is effective enough, the virus, in principle, should be eradicated.

We can estimate the required effectiveness of treatment from this condition. Under the assumption of a pretreatment steady state,  $c = NkT_0$ , and the stability condition becomes

$$\eta_{PI} > 1 - \frac{T_0}{T_{ss1}}.$$

Healthy individuals have T cell counts of about  $1000/\text{mm}^3$ . Thus, we can assume  $T_{ss1} = 1000$ . Hence for a patient with a pretreatment T cell count of, say,  $T_0 = 200$ , we find that  $\eta_{PI}$  needs to be greater than 0.8. For a less advanced patient with a T cell count of  $T_0 = 500$ ,  $\eta_{PI}$  need only be greater than 0.5. Thus, this analysis supports the notion that patients should be started on antiretroviral drug therapy as early as possible.

**5.5.3. Stability of the Infected Steady State.** This steady state exists only if  $\bar{V}_I > 0$  or if

$$(5.27) \quad \frac{s}{T_{ss2}} + p - d_T - p \frac{T_{ss2}}{T_{max}} > 0.$$

If the inequality (5.27) is replaced by an equality and the equation  $\bar{V}_I = 0$  is solved for  $T_{ss2}$ , we obtain an expression identical to the expression for  $T_{ss1}$ . Thus, at  $\bar{V}_I = 0$ , the uninfected and infected steady states merge. Further, as  $T_{ss2}$  decreases, the left-hand side of (5.27) increases. Hence, for  $\bar{V}_I > 0$  and the infected steady state to exist,  $0 < T_{ss2} < T_{ss1}$ . This makes biological sense since in the infected steady state the system should have fewer T cells than in the uninfected state.

Substituting the equation for  $T_{ss2}$  into the steady state equation for  $V_I$  gives a necessary condition for the infected steady state to exist, namely,

$$(5.28) \quad \bar{V}_I = \frac{sN(1 - n_{PI})}{c} + \frac{p \left( 1 - \frac{c}{NkT_{max}(1 - n_{PI})} \right) - d_T}{k} > 0.$$

The Jacobian matrix evaluated at this steady state is

$$\begin{pmatrix} p \left( 1 - \frac{2\bar{T}}{T_{max}} \right) - d_T - k\bar{V}_I & 0 & -k\bar{T} & 0 \\ k\bar{V}_I & -\delta & k\bar{T} & 0 \\ 0 & \delta N(1 - \eta_{PI}) & -c & 0 \\ 0 & \delta N \eta_{PI} & 0 & -c \end{pmatrix},$$

where  $\bar{T} = T_{ss2}$ .

The characteristic equation computed from this Jacobian has one factor of  $\lambda + c$ , implying  $\lambda_4 = -c$ . The other eigenvalues are the solutions of

$$\left[ p \left( 1 - 2 \frac{\bar{T}}{T_{max}} \right) - d_T - k\bar{V}_I - \lambda \right] [(c + \lambda)(\delta + \lambda) - k\bar{T}\delta N(1 - \eta_{PI})] - k\bar{V}_I k\bar{T}\delta N(1 - \eta_{PI}) = 0,$$

which, using the steady state value for  $\bar{T}$ , simplifies to

$$\lambda^3 + A\lambda^2 + B\lambda + C = 0,$$

where

$$\begin{aligned} A &= \delta + c + \left( \frac{2p\bar{T}}{T_{max}} \right) - (p - d_T) + k\bar{V}_I, \\ B &= (\delta + c) \left( \frac{2p\bar{T}}{T_{max}} - (p - d_T) + k\bar{V}_I \right), \\ C &= c\delta k\bar{V}_I. \end{aligned}$$

The Routh–Hurwitz conditions state that if  $A > 0$ ,  $C > 0$ , and  $AB - C > 0$ , then the eigenvalues have negative real parts. By inspection,  $C > 0$ . At steady state,

$$s + (p - d_T)\bar{T} - \frac{p\bar{T}^2}{T_{max}} = k\bar{V}_I\bar{T}.$$

Since  $s > 0$ ,

$$(p - d_T)\bar{T} - \frac{p\bar{T}^2}{T_{max}} < k\bar{V}_I\bar{T}$$

or

$$p - d_T < \frac{p\bar{T}}{T_{max}} + k\bar{V}_I,$$

from which it follows that  $A > 0$ . The remaining condition necessary for stability of the infected steady state is  $AB - C > 0$ . Note that  $A$  can be written as  $A = (\delta + c + B_1)$  and that  $B$  can be written as  $B = (\delta + c)B_1$ . Exploiting this form and noting that  $B_1$  contains the term  $k\bar{V}_I$ , one can show that  $AB = B_1(\delta + c)^2 + B_1^2(\delta + c) > \delta ck\bar{V}_I = C$ . Hence the infected steady state, if it exists, is stable.

Note that if the infected steady state exists,  $T_{ss2} < T_{ss1}$ , which we can rewrite as

$$c < NkT_{ss1}(1 - \eta_{PI}).$$

To summarize, if  $c > NkT_{ss1}(1 - \eta_{PI})$  then the only nonnegative steady state is the uninfected steady state and it is stable. Conversely, if  $c < NkT_{ss1}(1 - \eta_{PI})$  then the uninfected state is unstable and the infected state exists and is stable. This is equivalent to saying that there is a transcritical bifurcation when  $c = NkT_{ss1}(1 - \eta_{PI})$ .

**5.6. Viral Generation Time.** Virologists are interested in determining how rapidly virus replicates. One means of doing this is to estimate the generation time of the virus. Here we shall define the generation time of HIV as the time it takes a population of virions to infect cells and reproduce. Because a single virion may be cleared before it infects a cell, we cannot simply average the generation times of individual particles, for this average will diverge. The procedure we follow is to examine a steady state population of  $V_0$  virions in a patient with  $T = \text{constant} = T_0$  target cells. We then call the average time for this population to be replaced by a new population of  $V_0$  virions the generation time,  $T_g$ . Thus, for example, if the original virions are all colored red and newly produced virions are all colored blue, we compute the average time until the appearance of the new generation of  $V_0$  blue particles. While virions are not colored, the use of a 100% effective protease inhibitor causes newly produced virions to be noninfectious, i.e., blue. Because we wish to calculate the time until  $V_0$  noninfectious particles are created, we assume that such particles are not cleared and that initially none exist. Thus,  $dV_{NI}/dt = N\delta T^*$ , with  $V_{NI}(0) = 0$ . Further, we shall assume that at  $t = 0$  there are no productively infected cells so that only new infections are tracked. Thus,  $T^*(0) = 0$ , and from equation (5.13)

$$(5.29) \quad T^*(t) = \frac{kT_0V_0}{c - \delta}(e^{-\delta t} - e^{-ct}).$$

At any given time,  $t$ , the mean number of “blue” virions produced from the initial  $V_0$  “red” virions is  $V_{NI}(t)$ . If we let  $P(t)$  be the (cumulative) probability that a virion is produced by time  $t$ , then  $P(t) = V_{NI}(t)/V_0$ . The probability density of a virus being produced at time  $t$  is  $p(t) = dP/dt$ , and thus the average time of virion production is given by

$$(5.30) \quad T_g = \int_0^\infty tp(t)dt = \frac{1}{V_0} \int_0^\infty t \frac{dV_{NI}}{dt} dt = \frac{1}{V_0} \int_0^\infty tN\delta T^* dt.$$

Substituting the value of  $T^*(t)$  given above, using the quasi-steady state condition  $NkT_0 = c$ , and integrating, we find

$$(5.31) \quad T_g = \frac{1}{\delta} + \frac{1}{c}.$$

What we have called the viral generation time has a very simple interpretation. In the life cycle of HIV, virions are either free or within cells. The generation time is thus the sum of the average times spent in these two compartments,  $1/c$  being the average lifetime of a free virion and  $1/\delta$  being the average lifespan of an infected cell. There is also another interpretation. Because the system is at quasi-steady state,  $c = NkT_0$ , the clearance rate and rate of new cell infection are coupled. Thus, the viral generation time can also be viewed as the time for an infected cell to produce  $N$  new virions, i.e., its lifespan  $1/\delta$ , plus the time for this cohort of  $N$  virions to infect any of the  $T_0$  uninfected target cells, i.e.,  $1/(NkT_0)$ . For the five patients studied in [55], the average generation time was 2.6 days. In more recent studies employing combination therapy [51] or the RT inhibitor nevirapine [20], higher estimates of  $\delta$  were obtained, which lead to a generation time of 1.8 days. This implies that in a steady state patient, HIV goes through approximately 140 to 200 replication cycles per year.

**6. Drug Resistance.** The fact that  $> 10^{10}$  virions are produced each day in the average midstage HIV-1 infected patient has significant implications for the generation of drug resistance. When HIV replicates, its RNA genome is reverse transcribed into DNA. This copying process is error-prone, and in vivo the error rate has been estimated as  $3 \times 10^{-5}$  per base per replication cycle [36]. The HIV-1 genome has approximately  $10^4$  bases, and thus the average number of changes per genome is 0.3 per replication cycle. According to the binomial distribution or its Poisson approximation, we then expect, after one replication, 74% of infected cells to carry unmutated genomes, 22% of infected cells to carry genomes with one mutation, 3.3% to carry two mutations, 0.33% to carry three mutations, and so on (Table 6.1).

Not all  $10^{10}$  virions produced per day will infect other cells. Some will be defective; others, even if infectious, will be cleared. If, as suggested by Haase et al. [19], about 100 virions are produced per productively infected  $CD4^+$  T cell, then at steady state only one of these 100 virions should go on to successfully infect another cell and produce a new generation of virions. (Recent, unpublished data from P. Bucy, University of Alabama, suggests that this estimate of 100 virions may be an order of magnitude too low. However, even if true, it will not change the conclusions reached below.) If one productively infected cell led to the productive infection of more than one other cell, then the infection would not be in steady state and the number of virions would be increasing. If we assume that one out of a hundred virions infect another cell, then on average there are  $10^8$  new infections per day. Hence, as shown in Table 6.1, we expect on average  $0.22 \times 10^8$  mutants to be generated per day with single base changes. Because each of the  $10^4$  bases in HIV-1 could mutate to any of 3 other bases, there are a total of  $3^i \binom{n}{i}$  possible sequences of length  $n$  with  $i$  mutations. Thus, with  $n = 10^4$ , there are  $3 \times 10^4$  possible single base mutants, and essentially all of them would be generated each day. Consequently, resistance to drugs, such as 3TC, which only require a single base change is expected to occur rapidly and does [60]. In our initial studies with ritonavir [23], virus plasma levels fell to approximately 1% of their pretreatment values in 2 weeks. However, in 18 out of 20 patients the decrease in virus was not maintained for long periods, and the viral load rebounded. Genetic analysis suggests that one of the key resistance mutations for the protease gene, a valine to alanine substitution at position 82, preexisted [13], as predicted by these calculations. A similar pattern of rapid emergence of drug resistance to HIV-1 RT inhibitor nevirapine has also been seen [20, 65].

**Table 6.1** *Adapted from [52]. Assuming that the HIV genome is approximately  $10^4$  base pairs long and that RT introduces errors into the HIV genome at a rate of  $3 \times 10^{-5}$  per base pair per generation, the table shows the probability of an infected cell containing a proviral HIV genome with zero, one, two, or three mutations in it. Further, assuming  $10^8$  new cells are infected each day, the expected number of such mutants created each day within one infected individual is given. Lastly, we have also computed the fraction of all possible mutants with one, two, or three mutations that are created each day. If, for example, only one particular triple mutant gave rise to drug resistance then the probability of it being generated in a given patient on any given day from a wild-type virus is  $7.4 \times 10^{-8}$ .*

Base changes	Probability of mutant	Number created per day	Number of possible mutants	Fraction of all possible mutants created per day
0	0.74	$7.4 \times 10^7$	1	
1	0.22	$2.2 \times 10^7$	$3.0 \times 10^4$	1
2	0.033	$3.3 \times 10^6$	$4.5 \times 10^8$	$7.4 \times 10^{-3}$
3	0.0033	$3.3 \times 10^5$	$4.5 \times 10^{12}$	$7.4 \times 10^{-8}$

The chance of a mutant arising with a particular two-base change, while substantially lower, is not so low that it can be neglected. The rate of generation of double mutants is  $3.3 \times 10^6$ /day or  $\sim 0.74\%$ /day of the possible two-base mutants (Table 6.1). Because a number of mutation combinations can lead to resistance, there is a reasonable chance that two-base mutants that could confer drug resistance preexist or will appear. In fact, in a population of size  $1/7.4 \times 10^{-3} = 135$ , one would expect every possible double mutant to be created on average each day. Although we have not modeled mutant survival, we would expect many of these mutants to survive and be able to grow in the presence of drug. Thus, in a large population, many recipients of drug will show resistance if only two mutations are required. Models which explicitly take into consideration the generation and growth of mutants have been developed [3, 4, 47, 61, 66] and will not be reviewed here.

For three-base-change mutants, the situation is different. In single replication cycles, less than  $10^{-7}$  of all possible three-base mutants are generated per day (Table 6.1). Thus, it is extraordinarily unlikely that any particular three-base-change mutant will arise spontaneously. However, such mutants can be selected by sequential mutations if one- or two-base mutants replicate.

**7. Combination Therapy.** The results of the last section suggest that therapy using a single drug is doomed to fail because of drug resistance. Thus, in order to sustain a long-term response, models predict, and experience has borne out, that combination therapy is needed. Since both RT and protease inhibitors are available, most combination therapies employ both types of inhibitors in order to block the viral life cycle at two independent points.

In a clinical trial employing a protease inhibitor, nelfinavir, and two RT, AZT and 3TC, novel dynamics were observed after therapy was initiated [51]. As with a single drug, the virus concentration in plasma fell dramatically for one to two weeks. However, under continued therapy, after this initial “first phase” of decline, the virus continued to fall but at a significantly slower rate. When the virus concentration was plotted on a logarithmic scale, the two phases of viral decline were both seen to be approximately exponential, as displayed in Figure 7.1.

The question then arose: Why did the virus not continue to fall at the rapid first-phase rate? The antiretroviral effect of the combination therapy was potent in that the concentration of HIV-1 in plasma dropped below the standard detection threshold

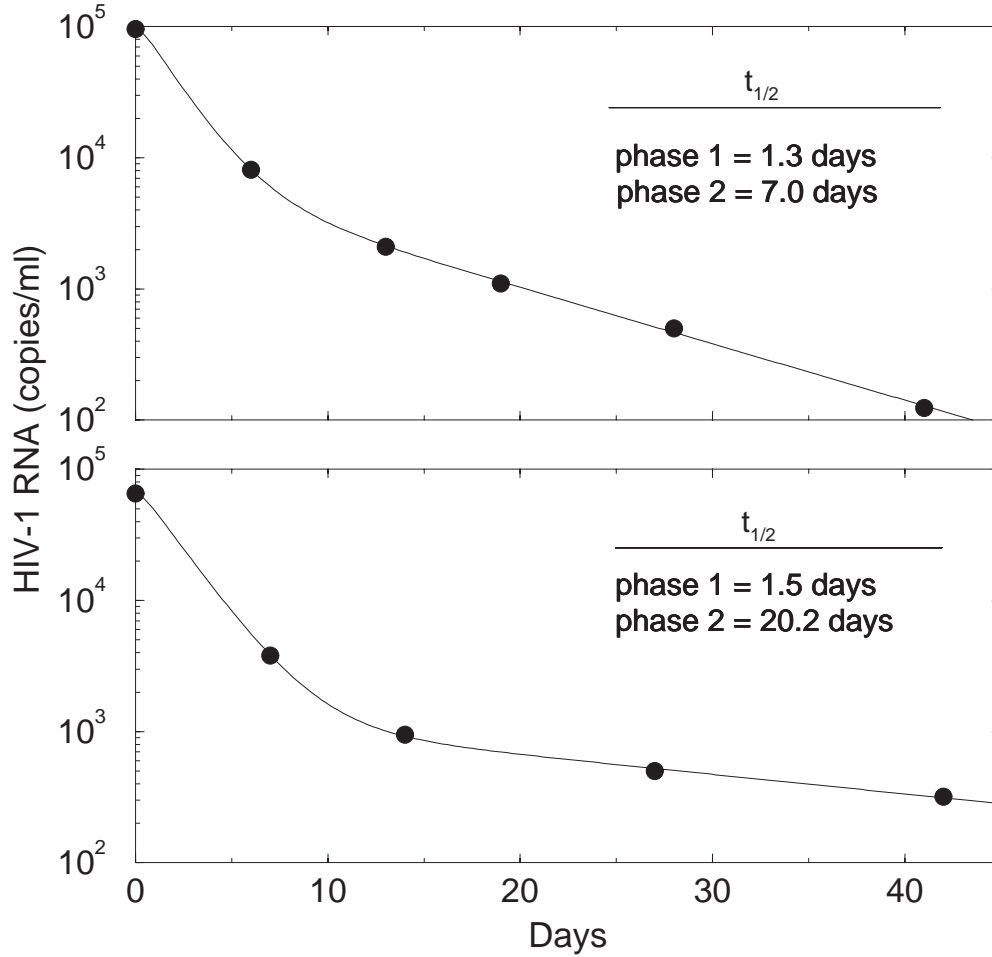


**Fig. 7.1** Examples of two-phase decline in plasma virus seen after the initiation of potent combination therapy. Data from two different patients is shown.

of 500 copies/ml by 8 weeks of treatment, and was found to be  $<25$  copies/ml at weeks 16–20 using an ultrasensitive assay. Further, there was no evidence of emergence of drug-resistant virus during the 16–20-week study period, suggesting that the second phase of decay has a biological origin.

In the presence of both RT and protease inhibitors our basic model, with  $T = \text{constant} = T_0$ , takes the form

$$(7.1) \quad \frac{dT^*}{dt} = (1 - \eta_{RT})kV_I T_0 - \delta T^*,$$

$$(7.2) \quad \frac{dV_I}{dt} = (1 - \eta_{PI})N\delta T^* - cV_I,$$

$$(7.3) \quad \frac{dV_{NI}}{dt} = \eta_{PI}N\delta T^* - cV_{NI},$$

where  $\eta_{RT}$  and  $\eta_{PI}$  are the effectiveness of the RT and protease inhibitors, respectively. If both the protease and RT inhibitors are 100% effective, then the model simplifies to

$$(7.4) \quad \frac{dT^*}{dt} = -\delta T^*,$$

$$(7.5) \quad \frac{dV_I}{dt} = -cV_I,$$

$$(7.6) \quad \frac{dV_{NI}}{dt} = N\delta T^* - cV_{NI},$$

with solution

$$T^*(t) = T^*(0)e^{-\delta t} = \frac{kV_0T_0}{\delta}e^{-\delta t},$$

$$V_I(t) = V_0e^{-ct},$$

$$V_{NI}(t) = \frac{N\delta T^*(0)}{c-\delta} [e^{-\delta t} - e^{-ct}].$$

If we assume that the patient was in quasi-steady state before treatment, then  $T^*(0) = kV_0T_0/\delta$  and  $NkT_0 = c$ , and we find

$$V(t) = V_I(t) + V_{NI}(t) = V_0 \left[ \frac{ce^{-\delta t} - \delta e^{-ct}}{c-\delta} \right].$$

Hence, one would expect that after a rapid transient of the order of  $1/c$ , the viral load would fall exponentially at a rate characterized by the constant  $\delta$ . This fall corresponds to the first-phase decline observed in the data.

Although there are many possible explanations for the second phase of plasma virus decline, we shall restrict our attention to those that we believe are the most plausible. First, if there were a source of virus other than infected cells, then the virus concentration, rather than falling continually, would ultimately come to a new steady state in which production by this source was in balance with clearance. If the source, rather than being constant, decayed slowly, then the virus concentration would exhibit a second phase decline whose rate reflected the rate of decay of the source.

In addition to  $CD4^+$  T cells, other cells are known to be susceptible to HIV-1 infection. One such pool of cells are macrophages, large cells that reside in tissue and which can engulf various biological debris. A fraction of these cells are  $CD4^+$ , and in cell culture they become productively infected by HIV-1. Furthermore, HIV infection in cell culture tends not to kill macrophages, and they are able to produce virus particles for weeks in culture. Another possibility is that the pool of T cells is heterogeneous, with a subpopulation of T cells upon infection producing fewer virions and living longer. Incorporating a second population of cells,  $M$ , susceptible to infection with rate constant  $k_M$ , we obtain the following, which we call the long-

lived infected cell model:

$$(7.7) \quad \frac{dT}{dt} = s + pT \left(1 - \frac{T}{T_{max}}\right) - d_T T - kVT,$$

$$(7.8) \quad \frac{dT^*}{dt} = kVT - \delta T^*,$$

$$(7.9) \quad \frac{dM}{dt} = s_M - d_M M - k_M VM,$$

$$(7.10) \quad \frac{dM^*}{dt} = k_M VM - \mu_M M^*,$$

$$(7.11) \quad \frac{dV}{dt} = N\delta T^* + p_M M^* - cV.$$

Here  $M^*$  denotes the concentration of productively infected long-lived cells, which are assumed to produce virus continually at rate  $p_M$  per cell and to die at rate  $\mu_M$  per cell. Long-lived cells are assumed to be created by a constant source at rate  $s_M$  and to die with rate constant  $d_M$ .

Before treatment is initiated we shall assume that patients are in quasi-steady state, so that at  $t = 0$ ,  $dV/dt = 0$ ,  $dT^*/dt = 0$ , and  $dM^*/dt = 0$ , or

$$(7.12) \quad T_0^* = kV_0T_0/\delta, \quad M_0^* = k_M V_0 M_0 / \mu_M, \quad N\delta T_0^* + p_M M_0^* = cV_0.$$

If both the protease and RT inhibitors are 100% effective, then for  $t > 0$ ,  $k = k_M = 0$ , and all virus that is produced is noninfectious. Hence, after therapy is initiated,

$$(7.13) \quad \frac{dT}{dt} = +pT \left(1 - \frac{T}{T_{max}}\right) - d_T T,$$

$$(7.14) \quad \frac{dT^*}{dt} = -\delta T^*,$$

$$(7.15) \quad \frac{dM}{dt} = s_M - d_M M,$$

$$(7.16) \quad \frac{dM^*}{dt} = -\mu_M M^*,$$

$$(7.17) \quad \frac{dV_I}{dt} = -cV_I,$$

$$(7.18) \quad \frac{dV_{NI}}{dt} = N\delta T^* + p_M M^* - cV_{NI}.$$

The equations for  $T$  and  $M$  decouple from the equations determining viral dynamics, and hence the assumption that  $T$  or  $M$  remains constant after therapy need not be

made. Because the viral dynamic equations are linear, the following solution can be obtained in a straightforward manner:

$$(7.19) \quad T^*(t) = T_0^* e^{-\delta t},$$

$$(7.20) \quad M^*(t) = M_0^* e^{-\mu_M t},$$

$$(7.21) \quad V_I(t) = V_0 e^{-ct},$$

$$(7.22) \quad V_{NI}(t) = \frac{N\delta T_0^*}{c - \delta} [e^{-\delta t} - e^{-ct}] + \frac{pM_0^*}{c - \mu_M} [e^{-\mu_M t} - e^{-ct}].$$

Using the quasi-steady state constraints (7.12), we find

$$V_{NI}(t) = V_0 \left[ \frac{NkT_0}{c - \delta} (e^{-\delta t} - e^{-ct}) + \frac{c - NkT_0}{c - \mu_M} (e^{-\mu_M t} - e^{-ct}) \right],$$

and hence

$$(7.23) \quad V(t) = V_0 \left[ \left( 1 - \frac{NkT_0}{c - \delta} - \frac{c - NkT_0}{c - \mu_M} \right) e^{-ct} + \frac{NkT_0}{c - \delta} e^{-\delta t} + \frac{c - NkT_0}{c - \mu_M} e^{-\mu_M t} \right].$$

Using nonlinear least squares regression we fitted the patient data obtained in this combination therapy clinical trial to the long-lived infected cell model and estimated three parameters:  $\delta$ ,  $\mu_M$ , and the composite parameter,  $NkT_0$ . Virion clearance occurred too rapidly to estimate  $c$  from the data obtained in this study. Thus  $c$  was held constant at the mean value,  $c = 3 \text{ day}^{-1}$ , determined in [55]. The parameter  $\mu_M$ , which determines the lifespan of the long-lived infected cells, ranged from 0.03 to 0.12  $\text{day}^{-1}$ , with a mean value of  $0.07 \pm 0.04 \text{ day}^{-1}$ . The half-life of the cell population responsible for the second phase of viral decay,  $t_{1/2} = \ln 2 / \mu_M$ , had a mean value of 13.3 days, with a standard deviation of 7.9 days. The theoretical curves generated from (7.23) using the best-fit parameter values gave an excellent fit to the data for all patients (see Figure 7.1 for examples). The values of  $\delta$  ranged from 0.36 to 0.81  $\text{day}^{-1}$ , with a mean of  $0.59 \pm 0.15 \text{ day}^{-1}$ . The corresponding  $t_{1/2}$  values of the short-lived infected cells ranged from 0.86 to 1.92 days, with a mean of  $1.25 \pm 0.34$  days. This mean value was somewhat smaller than our previous estimate of 1.6 days [55], possibly due to the greater effectiveness of the triple drug combination than the monotherapy used in [55].

While the long-lived cell model fits the patient data, it is not the only reasonable biological model. It is known that HIV-1 is trapped on the surface of follicular dendritic cells [8, 19, 21], a population of cells that reside in lymphoid tissue. HIV can also be released from these trapping sites [6]. Thus, the source underlying the second-phase kinetics might be the release of virions trapped in lymphoid tissue. Let  $V_L$  be the concentration of trapped virions. Such virions may be degraded within lymphoid tissue at rate  $\mu_{VL}$  per virion, or released into the circulation with rate constant  $p_M$ . Thus, once therapy starts, if we neglect any additional viral trapping, we obtain

$$(7.24) \quad \frac{dV_L}{dt} = -(\mu_{VL} + p_M)V_L.$$

Further, virus appears in the circulation at rate  $p_M V_L$ . Notice that if we let  $V_L = M^*$  and  $\mu_M = \mu_{VL} + p_M$ , then a model with productively infected short-lived  $CD4^+$  T cells and release of trapped virions would give rise to the same equations as the long-lived infected cell model for  $t > 0$ , and hence would make the same predictions as to how  $V(t)$  changes during therapy. Thus, the fact that one can obtain good agreement between experimental data and the long-lived cell model cannot be used to rule out release of trapped virions as an explanation or a part of the explanation for the second phase of viral decay.

One difference between the long-lived cell model and the trapped virion model is that virions released from tissues would be virions trapped before therapy was initiated and hence should be infectious rather than noninfectious. Thus, it might be possible to distinguish this model from the long-lived cell model experimentally. So far, this has not been possible due to technical difficulties in analyzing the low concentration of virions that can be obtained during the second phase. The models could also be distinguished if trapping of virions were occurring at an observable rate during therapy. We are currently examining more detailed models of viral transport between blood and lymphoid tissue, with reversible binding of virus particles to follicular dendritic cells.

Another alternative model is one based on the activation of latently infected cells,  $L$ . Recall that latently infected cells are cells that harbor HIV-1 DNA as a provirus but which are not producing virus. These cells, when activated into cell division, reproduce their DNA, and in the process they read the viral DNA. Due to signals embedded in the viral genetic code this may cause the production of new virus particles. Hence, the activation of latently infected cells can turn them into productively infected cells.

To model the process of latent infection, we assume that when  $CD4^+$  T cells,  $T$ , are infected,  $T^*$  cells are produced with rate constant  $k$  and that latently infected cells are produced with rate constant  $fk$ , with  $f < 1$ . Latently infected cells are assumed to die at rate  $\delta_L$  and to be activated at rate  $a$ , giving a total rate of loss  $\mu_L = a + \delta_L$ . According to this model,

$$\begin{aligned} \frac{dT}{dt} &= s + pT \left(1 - \frac{T}{T_{max}}\right) - d_T T - kVT, \\ \frac{dT^*}{dt} &= kVT + aL - \delta T^*, \\ \frac{dL}{dt} &= fkVT - \mu_L L, \\ \frac{dV}{dt} &= N\delta T^* - cV. \end{aligned}$$

Again assuming the RT and protease inhibitors in the combination are 100% effective (so that for  $t > 0$ ,  $k = 0$ ), and that the patient is in quasi-steady state before therapy (so that at  $t = 0$ ,  $dT^*/dt = dL/dt = dV/dt = 0$ ), one finds that

$$(7.25) \quad V = V_0 [Ae^{-\delta t} + Be^{-\mu_L t} + (1 - A - B)e^{-ct}],$$

where

$$A = \frac{c\mu_L}{(\mu_L + af)(c - \delta)} \left(1 - \frac{af}{\delta - \mu_L}\right),$$

$$B = \frac{af\delta c}{(\mu_L + af)(c - \mu_L)(\delta - \mu_L)}.$$

Fitting the latently infected cell model to the patient data provided estimates of  $\delta$  and  $\mu_L$ . However, the data was not sufficient to separately determine the other parameters in the coefficients  $A$  and  $B$ .

The parameter  $\mu_L$  determines the rate of loss of latently infected cells, by either death or activation. The best-fit values of  $\mu_L$  were indistinguishable from the best-fit values of  $\mu_M$  determined in the long-lived infected cell model, and correspond to the slope of the second-phase decay. Examining the relationship between the values of  $\mu_M$ , or  $\mu_L$ , with the patient's baseline CD4 count, we found an inverse correlation. Thus, the lower the baseline CD4 count, the faster the cells responsible for the second phase of viral decay are lost. This is not what one would expect if such cells were being eliminated by a host immune response. Within the context of the latently infected cell model, the increase in  $\mu_L$  may reflect an increase in the rate of cell activation,  $\mu_L = a + \delta_L$ , with disease progression [58].

The latently infected cell model also gives predictions for the best-fit value of  $\delta$ , the short-lived infected cell lifetime, that are indistinguishable from the values obtained from the long-lived infected cell model. Using the best-fit parameter values, the theoretical curves predicted from (7.25) are indistinguishable from those predicted by (7.23). Hence, both the latently infected cell model and the long-lived infected cell model make identical predictions for the course of second-phase decay. However, the two models can be distinguished by the use of additional experimental information.

In a system where a population of latently infected cells is responsible for the second phase of viral decay, an increase in the activation rate of resting cells could significantly alter the decay behavior. Such an increase could be caused by, for example, natural infection, vaccination, or artificial stimulation of the immune system by some type of immunotherapy. Thus, immune stimulation administered during the second phase of viral decay for a patient with inhibitor effectiveness approaching 100% could provide important information concerning the mechanism of viral decay. Following a significant immunogenic challenge, the latently infected cell model predicts an increase in viral burden followed by an accelerated decay and subsequent clearance of infection, or a return to second-phase-type decay, depending on the magnitude of the immunogenic challenge as shown in Figure 7.2, while the long-lived productively infected cell model predicts no change in the slow second-phase decay. Preliminary experiments in which patients were vaccinated during the second phase did not show a statistically significant increase in viral load. Further experiments are planned in which more potent immunostimulation is given.

We have shown that measuring the viral load in blood after initiation of antiretroviral treatment does not provide sufficient information to identify the biological processes underlying the second phase of viral decline. This conclusion, which was taken seriously by our experimental collaborator David Ho, led to the performance of the following additional experiment. Blood, in addition to containing virus particles, also contains infected cells. The number of such cells can be estimated by limiting dilution procedures [34]. A fixed number of cells are taken from a patient and placed in cell culture with T cells from a healthy donor. If the culture conditions are proper, then if there are any infected cells in the patient sample, the T cells in the culture should become infected. Placing successively fewer patient cells in similar cultures, one ultimately finds that at some limited number of cells, the cultures do

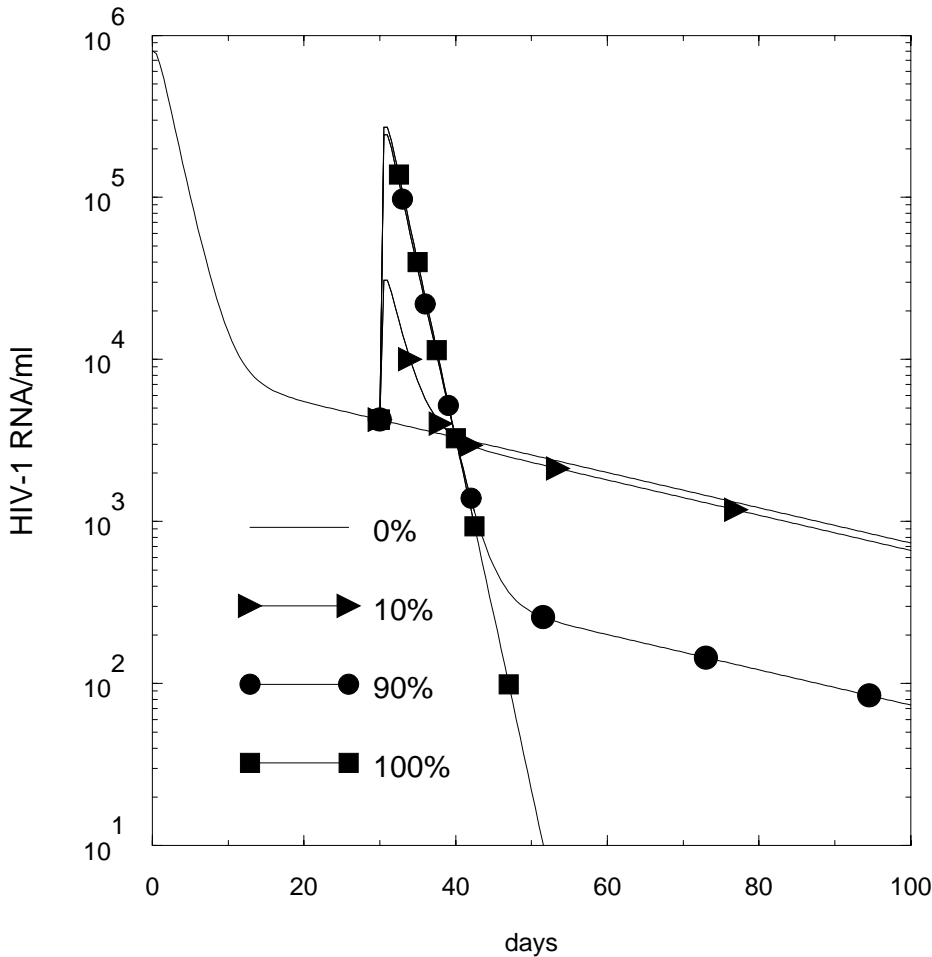


**Fig. 7.2** Predictions of the effects of immune stimulation from the latently infected cell model. At  $t = 30$  days, a fraction of latently infected cells are converted into productively infected cells,  $T^*$ . The figure shows that large perturbations would be needed to see a substantial change in viral load.

not become infected. Upon running the assays multiple times and doing a proper statistical analysis, quantitative estimates can be obtained for the expected frequency of infected cells.

In the limiting dilution cultures, latently infected cells should become activated and produce virus. Thus the number of infected cells detected by these limiting dilution procedures should be equal to the number of productively infected T cells,  $T^*$ , plus the number of latently infected cells capable of making virus,  $L$ . (Latently infected cells that are not capable of producing virus can be ignored since they cannot contribute to the second phase of viral decay.) Long-lived cells such as macrophages reside in tissue, and thus it is sensible to assume that they are not detected in the limiting dilution assay, which uses a sample of cells from blood as starting material.

Using this logic, as well as limiting dilution data, Perelson et al. [51] analyzed a model in which both latently infected and long-lived cells were included. This

combined model had the obvious form:

$$\begin{aligned}
 \frac{dT}{dt} &= s + pT \left(1 - \frac{T}{T_{max}}\right) - d_T T - kVT, \\
 \frac{dT^*}{dt} &= kVT + aL - \delta T^*, \\
 \frac{dL}{dt} &= fkVT - \mu_L L, \\
 \frac{dM}{dt} &= s_M - d_M M - k_M VM, \\
 \frac{dM^*}{dt} &= k_M VM - \mu_M M^*, \\
 \frac{dV}{dt} &= N\delta T^* + p_M M^* - cV,
 \end{aligned}
 \tag{7.26}$$

and solution

$$V(t) = V_0[Ae^{-\delta t} + Be^{-\mu_L t} + Ce^{-\mu_M t} + (1 - A - B - C)e^{-ct}],
 \tag{7.27}$$

where

$$\begin{aligned}
 A &= \frac{NkT_0}{c - \delta} \left(1 - \frac{af}{\delta - \mu_L}\right), \\
 B &= \frac{af\delta NkT_0}{\mu_L(\delta - \mu_L)(c - \mu_L)}, \\
 C &= \frac{c - NkT_0 \left(1 + \frac{af}{\mu_L}\right)}{c - \mu_M},
 \end{aligned}$$

where we again have assumed a pretreatment quasi-steady state and 100% effective treatment. Further, the limiting dilution data was assumed to give the frequency of infected cells, a quantity assumed to be proportional to  $I(t) \equiv T^*(t) + L(t)$ . From the solution of (7.26), one easily obtains

$$I(t) = \frac{kV_0T_0}{\delta} \left[ \left(1 - \frac{af}{\delta - \mu_L}\right) e^{-\delta t} + \frac{f\delta}{\mu_L} \left(1 + \frac{a}{\delta - \mu_L}\right) e^{-\mu_L t} \right].
 \tag{7.28}$$

Fitting experimental data to the combined model gave estimates of the most important parameters. Details can be found in [51]. This analysis suggested that while both latently infected and long-lived cells contribute to the second phase, long-lived infected cells are the major source of second-phase virus. Estimating the total possible body burden of long-lived infected cells to be between  $10^9$  and  $10^{12}$ , and assuming that the second phase decays with a half-life of four weeks, the slowest rate among the patients studied in [51], we estimated that on average it would take between two and a half and three years of perfectly effective treatment to allow the cells responsible for the second phase to completely decay, and for  $V$  to approach

zero in this model. These estimates, when presented in preliminary form at the XIth International Conference on AIDS in Vancouver in 1996 [53], generated a lot of enthusiasm and optimism. It was hoped that, if patients were kept on drugs for two to three years, the virus might be eradicated. More importantly, it established that even though the amount of viral RNA went undetectable in patients after some months of combination therapy, patients need to remain on therapy for at least a few years to allow the cells responsible for the second phase to decay.

**8. Discussion.** In this paper we have tried to show how mathematical modeling has impacted our understanding of HIV pathogenesis. Before modeling was brought to bear in a serious manner, AIDS was thought to be a slow disease in which treatment could be delayed until symptoms appeared, and patients were not monitored very aggressively. In the large, multicenter AIDS cohort studies aimed at monitoring the natural history of the disease, blood typically was drawn every six months. There was a poor understanding of the biological processes that were responsible for the observed levels of virus in the blood and the rapidity at which the virus became drug resistant. Modeling, coupled with advances in technology, has changed all of this. In section 2, we showed how an extremely simple model involving a single linear ordinary differential equation, when applied to the interpretation of clinical data obtained in a phase I/II drug trial, gave the first quantitative estimate of how rapidly HIV was being produced and cleared in an infected person. While the mathematics involved was trivial, the application of mathematics in this manner was novel and set off what has been described as a revolution in thinking about HIV. The papers by Ho et al. [23] and Wei et al. [65] that were published in the same issue of *Nature* and that both reported an approximately two-day half-life for HIV in plasma, were the most highly cited scientific papers published in 1995.

A more complex model presented in section 3 that incorporated both virus and infected cells, when compared with data collected to test the model, showed that the two-day viral half-life mainly reflected the lifetime of infected cells that produced virus. Thus, the first estimate of the lifetime of a productively infected cell in vivo was obtained, which allowed us to think in a more quantitative manner about the issue of  $CD4^+$  T cell depletion, the hallmark of AIDS. Further, the estimate of the rate of clearance of free viral particles was improved and the half-life of free virus particles in plasma is now estimated at six hours or less. Because the level of virus is maintained at steady state, the rate of viral clearance can be used to determine how rapidly HIV is produced. Doing these calculations led to the conclusion that in an average HIV-infected person, at least  $10^{10}$  virus particles are produced and released into bodily fluids each day. As explained in section 5.6, these estimates can be used to calculate a viral generation time of approximately 1.8 days. This implies that in an infected person HIV can go through about 200 replication cycles per year, with the possibility of mutating at each replication. Thus, the rapid evolution of HIV can easily be understood. The practical implication of this was that therapy with a single drug in which a few mutations were all that were required for resistance to arise could be shown to be a poor strategy. This helped usher in the current strategy of combination therapy and the approach of treating HIV-infected persons as soon after diagnosis as possible.

Using more complex models, involving multiple cell populations, has allowed further interpretation of clinical data obtained from patients on combination therapy, in which the virus concentration in plasma has a two-phase decline. This work, described in section 7, has also had important practical consequences. By extrapolating in a

rigorous way the data obtained from patients responding well to combination therapy, we were able to estimate how long therapy would need to be given to clear the cells responsible for producing the observed levels of virus. While bringing home the lesson that therapy would need to continue for years after free virus became undetectable in blood, the work also began the process of quantifying both the level and the role of latently infected and long-lived infected cell populations in HIV infection.

Throughout this paper we have analyzed situations in which models predict that under sufficiently intense therapy, the virus and infected cell concentrations will go to zero. The question then arises: Is viral eradication a realistic expectation? At the moment, we do not know. Clearly, the models that we have analyzed are only simplified caricatures of reality. They have not included the spatial and compartmental aspects of the body, and have implicitly assumed that drug is available everywhere in the body at a constant effectiveness. Not all drugs penetrate the blood–brain barrier effectively, and thus drug concentrations in the brain and central nervous system tend to be lower than in the circulation. Also, the cells of the immune system have limited access to these sites, and hence the brain and other sites with poor drug penetrance, such as the testes, may act as sanctuaries for the virus. Not surprisingly, in models with drug sanctuaries it is easier to generate drug resistance [28], and hence ongoing viral replication may remain a problem until a new generation of drugs becomes available.

The models have only dealt with the major targets of HIV infection,  $CD4^+$  T cells and macrophages. However, other cells may become HIV-infected and exhibit different kinetics. We have only dealt with infection of cells by free virus and the death of cells due to viral infection. Direct cell-to-cell transmission of virus has been reported in cell culture, as has death of cells due to effects other than direct viral killing. All of these features may play a role in the long-term behavior of HIV-1 in vivo.

Another large omission in our models has been the immune response. Processes such as the death of virally infected cells and/or the clearance of free viral particles may have an immune component. Furthermore, viruses can evolve to become more pathogenic and drug resistant. Thus, parameters in our models, rather than being constant, as we have assumed, may vary in time and depend in some complex way on events occurring in the host. Many of us hope that drugs will not need to be given until every last viral particle and infected cell is eliminated, but rather that as the amount of virus is reduced by antiretroviral drugs, recovery of the immune system will occur, and the host defense system will ultimately be able to control or clear any remaining virus. Both models and experiment are needed to examine this possibility.

Potent combination therapy has been available for 2 to 3 years. Analysis of lymphocytes from blood and tissue biopsies have shown that small numbers of latently infected cells can be found in patients treated for as long as 2.5 years [16, 69]. Whether the immune system can control the remaining infection is not known, and thus cessation of antiretroviral treatment is not recommended. The rate at which latently infected cells are decaying, and particularly those carrying proviruses that can generate infectious particles on stimulation, is also not yet known, although there are some suggestions that they may have a half-life of approximately 3 to 5 months [22]. Making estimates of the pool size of latently infected cells, one can surmise that 5 to 7 years of continuous therapy may be required to achieve eradication of latently infected  $CD4^+$  T cells [22]. This is an unacceptable solution due to the complex-

ity of complying with current drug regimes, drug side effects, and cost. Alternative approaches are needed and are being examined [22].

Models, such as the ones discussed here, have been developed and tested on data obtained over relatively short periods: days, weeks, and in some cases months. Even though the models appear accurate on these time scales, they should not be used to predict the long-term events in individual patients. They have provided much insight into the biological events underlying the disease process and have helped guide treatment strategies. Eradicating HIV from an infected patient or helping the body control the infection still remains our goal. We believe that modeling will continue to play an important role in attaining this goal.

**Acknowledgments.** This work would not have been possible without extensive collaboration with David D. Ho, head of the Aaron Diamond AIDS Research Center, Rockefeller University, New York. Dr. Martin Markowitz, Aaron Diamond AIDS Research Center, was responsible for the clinical aspects of the studies reported here. Avidan Neumann of Bar-Ilan University, Israel and Paulina Essunger of Harvard University contributed to the original analysis of the patient data. We thank Lee Segel for reading and commenting on the manuscript.

#### REFERENCES

- [1] R. M. ANDERSON AND R. M. MAY, *Epidemiology parameters of HIV transmission*, Nature, 333 (1988), pp. 514–519.
- [2] R. W. ANDERSON, M. S. ASCHER, AND H. W. SHEPPARD, *Direct HIV cytopathicity cannot account for CD4 decline in AIDS in the presence of homeostatis: A worst-case dynamic analysis*, J. AIDS and Human Retrovirol., 17 (1998), pp. 245–252.
- [3] S. BONHOEFFER, R. M. MAY, G. M. SHAW, AND M. A. NOWAK, *Virus dynamics and drug therapy*, Proc. Nat. Acad. Sci. U.S.A., 94 (1997), pp. 6971–6976.
- [4] S. BONHOEFFER AND M. A. NOWAK, *Pre-existence and emergence of drug resistance in HIV-1 infection*, Proc. Roy. Soc. London B, 264 (1997), pp. 631–637.
- [5] A. CARMICHAEL, X. JIN, P. SISSONS, AND L. BORYSIEWICZ, *Quantitative analysis of the human immunodeficiency virus type 1 (HIV-1)-specific cytotoxic T lymphocyte (CTL) response at different stages of HIV-1 infection: Differential CTL responses to HIV-1 and Epstein-Barr virus in late disease*, J. Exp. Med., 177 (1993), pp. 249–256.
- [6] W. CAVERT, D. W. NOTERMANS, K. STASKUS, S. W. WIETGREFE, M. ZUPANCIC, K. GEBHARD, K. HENRY, Z. Q. ZHANG, R. MILLS, H. MCDADE, C. M. SCHUWIRTH, J. GOUDSMIT, S. A. DANNER, AND A. T. HAASE, *Kinetics of response in lymphoid tissues to antiretroviral therapy of HIV-1 infection*, Science, 276 (1997), pp. 960–964.
- [7] T. W. CHUN, L. CARRUTH, D. FINZI, X. SHEN, J. A. DIGIUSEPPE, H. TAYLOR, M. HERMANKOVA, K. CHADWICK, J. MARGOLICK, T. C. QUINN, Y. H. KUO, R. BROOKMEYER, M. A. ZEIGER, P. BARDITCH-CROVO, AND R. F. SILICIANO, *Quantification of latent tissue reservoirs and total body viral load in HIV-1 infection*, Nature, 387 (1997), pp. 183–188.
- [8] E. A. CLARK, *HIV: Dendritic cells as embers for the infectious fire*, Current Biology, 6 (1996), pp. 655–657.
- [9] J. M. COFFIN, *HIV population dynamics in vivo: Implications for genetic variation, pathogenesis, and therapy*, Science, 267 (1995), pp. 483–489.
- [10] L. N. COOPER, *Theory of an immune system retrovirus*, Proc. Nat. Acad. Sci. U.S.A., 83 (1986), pp. 9159–9163.
- [11] R. J. DE BOER AND A. S. PERELSON, *Target cell limited and immune control models of HIV infection: A comparison*, J. Theoret. Biol., 190 (1998), pp. 201–214.
- [12] J. DOLEZAL AND T. HRABA, *Application of mathematical model of immunological tolerance to HIV infection*, Folia Biol., 34 (1988), pp. 336–341.
- [13] P. S. EASTMAN, J. E. MITTLER, R. KELSO, C. GEE, E. BOYER, J. KOLBERG, M. URDEA, J. M. LEONARD, D. W. NORBECK, H. MO, AND M. MARKOWITZ, *Genotypic changes in human immunodeficiency virus type 1 associated with loss of suppression of plasma viral RNA*

- levels in subjects treated with ritonavir (norvir) monotherapy, *J. Virology*, 72 (1998), pp. 5154–5164.
- [14] P. ESSUNGER, M. MARKOWITZ, D. D. HO, AND A. S. PERELSON, *Efficacy of drug combination and dosing regimen in antiviral therapy*, in Intl. Workshop on HIV Drug Resistance, Treatment Strategies and Eradication, St. Petersburg, FL, June 1997, Antiviral Therapy, Abstr. 73, 1997.
- [15] P. ESSUNGER AND A. S. PERELSON, *Modeling HIV infection of CD4+ T-cell subpopulations*, *J. Theoret. Biol.*, 170 (1994), pp. 367–391.
- [16] D. FINZI, M. HERMANKOVA, T. PIERSON, L. M. CARRUTH, C. BUCK, R. E. CHAISSON, T. C. QUINN, K. CHADWICK, J. MARGOLICK, R. BROOKMEYER, J. GALLANT, M. MARKOWITZ, D. D. HO, D. D. RICHMAN, AND R. F. SILICIANO, *Identification of a reservoir for HIV-1 in patients on highly active antiretroviral therapy*, *Science*, 278 (1997), pp. 1295–1300.
- [17] S. D. W. FROST AND A. R. MCLEAN, *Germinal centre destruction as a major pathway of HIV pathogenesis*, *J. AIDS*, 7 (1994), pp. 236–244.
- [18] S. D. W. FROST AND A. R. MCLEAN, *Quasispecies dynamics and the emergence of drug resistance during zidovine therapy of HIV infection*, *AIDS*, 8 (1994), pp. 323–332.
- [19] A. T. HAASE, K. HENRY, M. ZUPANCIC, G. SEDGEWICK, R. A. FAUST, H. MELROE, W. CAVERT, K. GEBHARD, K. STASKUS, Z. Q. ZHANG, P. J. DAILEY, H. H. BALFOUR JR, A. ERICE, AND A. S. PERELSON, *Quantitative image analysis of HIV-1 infection in lymphoid tissue*, *Science*, 274 (1996), pp. 985–989.
- [20] D. V. HAVLIR, S. EASTMAN, A. GAMST, AND D. D. RICHMAN, *Nevirapine-resistant human immunodeficiency virus: Kinetics of replication and estimated prevalence in untreated patients*, *J. Virol.*, 70 (1996), pp. 7894–7899.
- [21] S. L. HEATH, J. G. TEW, A. K. SZAKAL, AND G. F. BURTON, *Follicular dendritic cells and human immunodeficiency virus infectivity*, *Nature*, 377 (1995), pp. 740–744.
- [22] D. D. HO, *Toward HIV eradication or remission: The tasks ahead*, *Science*, 280 (1998), pp. 1866–1867.
- [23] D. D. HO, A. U. NEUMANN, A. S. PERELSON, W. CHEN, J. M. LEONARD, AND M. MARKOWITZ, *Rapid turnover of plasma virions and CD4 lymphocytes in HIV-1 infection*, *Nature*, 373 (1995), pp. 123–126.
- [24] D. D. HO, R. J. POMERANTZ, AND J. C. KAPLAN, *Pathogenesis of infection with human immunodeficiency virus*, *New England J. Med.*, 317 (1987), pp. 278–286.
- [25] T. HRABA AND J. DOLEZAL, *Mathematical model of CD4+ lymphocyte depletion in HIV infection*, *Folia Biol.*, 35 (1989), pp. 156–163.
- [26] T. HRABA, J. DOLEZAL, AND S. CELIKOVSK'Y, *Model-based analysis of CD4+ lymphocytes dynamics in HIV infected individuals*, *Immunobiology*, 181 (1990), pp. 108–118.
- [27] N. INTRATOR, G. P. DEOCAMPO, AND L. COOPER, *Analysis of immune system retrovirus equations*, in *Theoretical Immunology, Part 2*, A. S. Perelson, ed., Addison-Wesley, Redwood City, CA, 1988.
- [28] T. B. KEPLER AND A. S. PERELSON, *Drug concentration heterogeneity facilitates the evolution of drug resistance*, *Proc. Nat. Acad. Sci. U.S.A.*, 95 (1998), pp. 11514–11519.
- [29] D. KIRSCHNER, *Using mathematics to understand HIV immune dynamics*, *Notices Amer. Math. Soc.*, 43 (1996), pp. 191–202.
- [30] D. KIRSCHNER, S. LENHART, AND S. SERBIN, *Optimal control of the chemotherapy of HIV*, *J. Math. Biol.*, 35 (1997), pp. 775–792.
- [31] D. E. KIRSCHNER, R. MEHR, AND A. S. PERELSON, *The role of the thymus in pediatric HIV-1 infection*, *J. AIDS Human Retroviro.*, 18 (1998), pp. 95–109.
- [32] D. E. KIRSCHNER AND G. F. WEBB, *A model for treatment strategy in the chemotherapy of AIDS*, *Bull. Math. Biol.*, 58 (1996), pp. 367–391.
- [33] D. E. KIRSCHNER AND G. F. WEBB, *Understanding drug resistance for monotherapy treatment of HIV infection*, *Bull. Math. Biol.*, 59 (1997), pp. 763–785.
- [34] I. LEFKOVITS AND H. WALDMANN, *Limiting Dilution Analysis of Cells in the Immune System*, Cambridge University Press, Cambridge, UK, 1979.
- [35] R. LEONARD, D. ZAGURY, I. DESPORTES, J. BERNARD, J. F. ZAGURY, AND R. C. GALLO, *Cytopathic effect of human immunodeficiency virus in T4 cells is linked to the last stage of virus infection*, *Proc. Nat. Acad. Sci. U.S.A.*, 85 (1988), pp. 3570–3574.
- [36] L. M. MANSKY AND H. M. TEMIN, *Lower in vivo mutation rate of human immunodeficiency virus type 1 than that predicted from the fidelity of purified reverse transcriptase*, *J. Virol.*, 69 (1995), pp. 5087–5094.
- [37] A. R. MCLEAN, *HIV infection from an ecological viewpoint*, in *Theoretical Immunology, Part 2*, A. S. Perelson, ed., Addison-Wesley, Redwood City, CA, 1988.

- [38] A. R. McLEAN AND S. D. W. FROST, *Zidovudine and HIV: Mathematical models of within-host population dynamics*, Rev. Med. Virol., 5 (1995), pp. 141–147.
- [39] A. R. McLEAN AND T. L. B. KIRKWOOD, *A model of human immunodeficiency virus (HIV) infection in T-helper cell clones*, J. Theoret. Biol., 147 (1990), pp. 177–203.
- [40] A. R. McLEAN AND M. A. NOWAK, *Models of interactions between HIV and other pathogens*, J. Theoret. Biol., 155 (1992), pp. 69–86.
- [41] S. MERRILL, *AIDS: Background and the dynamics of the decline of immunocompetence*, in Theoretical Immunology, Part 2, A. S. Perelson, ed., Addison-Wesley, Redwood City, CA, 1988.
- [42] S. MERRILL, *Modeling the interaction of HIV with the cells of the immune system*, in Mathematical and Statistical Approaches to AIDS Epidemiology, Lecture Notes in Biomath. 83, Springer-Verlag, New York, 1989.
- [43] H. MOHRI, S. BONHOEFFER, S. MONARD, A. S. PERELSON, AND D. D. HO, *Rapid turnover of T lymphocytes in SIV-infected rhesus macaques*, Science, 279 (1998), pp. 1223–1227.
- [44] M. A. NOWAK, *Variability of HIV infections*, J. Theoret. Biol., 155 (1992), pp. 1–20.
- [45] M. A. NOWAK, R. M. ANDERSON, M. C. BOERLIJST, S. BONHOEFFER, R. M. MAY, AND A. J. MCMICHAEL, *HIV-1 evolution and disease progression*, Science, 274 (1996), pp. 1008–1010.
- [46] M. A. NOWAK, R. M. ANDERSON, A. R. McLEAN, T. F. W. WOLFS, J. GOUDSMIT, AND R. M. MAY, *Antigenic diversity threshold and the development of AIDS*, Science, 254 (1991), pp. 963–969.
- [47] M. A. NOWAK, S. BONHOEFFER, G. M. SHAW, AND R. M. MAY, *Anti-viral drug treatment: Dynamics of resistance in free virus and infected cell populations*, J. Theoret. Biol., 184 (1997), pp. 205–219.
- [48] M. A. NOWAK AND R. M. MAY, *Mathematical biology of HIV infections: Antigenic variation and diversity threshold*, Math. Biosci., 106 (1991), pp. 1–21.
- [49] A. S. PERELSON, *Modeling the interaction of HIV with the immune system*, in Mathematical and Statistical Approaches to AIDS Epidemiology, Lecture Notes in Biomath., 83, Springer-Verlag, New York, 1989.
- [50] A. S. PERELSON, *Two theoretical problems in immunology: AIDS and epitopes*, in Complexity: Metaphors, Models and Reality, G. Cowan, D. Pines, and D. Meltzer, eds., Addison-Wesley, Reading, CA, 1994.
- [51] A. S. PERELSON, P. ESSUNGER, Y. CAO, M. VESANEN, A. HURLEY, K. SAKSELA, M. MARKOWITZ, AND D. D. HO, *Decay characteristics of HIV-1-infected compartments during combination therapy*, Nature, 387 (1997), pp. 188–191.
- [52] A. S. PERELSON, P. ESSUNGER, AND D. D. HO, *Dynamics of HIV-1 and CD4+ lymphocytes in vivo*, AIDS, 11 (suppl A) (1997), pp. S17–S24.
- [53] A. S. PERELSON, P. ESSUNGER, M. MARKOWITZ, AND D. D. HO, *How long should treatment be given if we had an antiretroviral regimen that completely blocked HIV replication?*, in XIth Intl. Conf. on AIDS Abstracts, 1996.
- [54] A. S. PERELSON, D. E. KIRSCHNER, AND R. DE BOER, *Dynamics of HIV infection of CD4+ T cells*, Math. Biosci., 114 (1993), pp. 81–125.
- [55] A. S. PERELSON, A. U. NEUMANN, M. MARKOWITZ, J. M. LEONARD, AND D. D. HO, *HIV-1 dynamics in vivo: Virion clearance rate, infected cell life-span, and viral generation time*, Science, 271 (1996), pp. 1582–1586.
- [56] A. N. PHILLIPS, *Reduction of HIV concentration during acute infection: Independence from a specific immune response*, Science, 271 (1996), pp. 497–499.
- [57] G. REIBNEGGER, D. FUCHS, A. HAUSEN, E. R. WERNER, M. P. DIERICH, AND H. WACHTER, *Theoretical implications of cellular immune reactions against helper lymphocytes infected by an immune system retrovirus*, Proc. Nat. Acad. Sci. U.S.A., 84 (1987), pp. 7270–7274.
- [58] N. SACHSENBERG, A. S. PERELSON, S. YERLY, G. A. SCHOCKMEL, D. LEDUC, B. HIRSCHL, AND L. PERRIN, *Turnover of CD4+ and CD8+ T lymphocytes in HIV-1 infection as measured by ki-67 antigen*, J. Exp. Med., 187 (1998), pp. 1295–1303.
- [59] D. SCHENZLE, *A model for AIDS pathogenesis*, Stat. Med., 13 (1994), pp. 2067–2079.
- [60] R. SCHUURMAN, M. NIJHUIS, R. VAN-LEEUEWEN, P. SCHIPPER, D. DE-JONG, P. COLLIS, S. A. DANNER, J. MULDER, C. LOVEDAY, AND C. CHRISTOPHERSON, *Rapid changes in human immunodeficiency virus type 1 RNA load and appearance of drug-resistant virus populations in persons treated with lamivudine (3TC)*, J. Infect. Dis., 171 (1995), pp. 1411–1419.
- [61] N. I. STILIANAKIS, C. A. B. BOUCHER, M. D. DEJONG, R. VAN-LEEUEWEN, R. SCHUURMAN, AND R. J. DEBOER, *Clinical data sets on human immunodeficiency virus type 1 reverse transcriptase resistant mutants explained by a mathematical model*, J. Virol., 71 (1997), pp. 161–168.

- [62] N. I. STILIANAKIS, K. DIETZ, AND D. SCHENZLE, *Analysis of a model for the pathogenesis of AIDS*, Math. Biosci., 145 (1997), pp. 27–46.
- [63] N. I. STILIANAKIS, D. SCHENZLE, AND K. DIETZ, *On the antigenic diversity threshold model for AIDS*, Math. Biosci., 121 (1994), pp. 235–247.
- [64] W. Y. TAN AND H. WU, *Stochastic modeling of the dynamics of CD4<sup>+</sup> T-cell infection by HIV and some Monte Carlo studies*, Math. Biosci., 147 (1997), pp. 173–205.
- [65] X. WEI, S. K. GHOSH, M. E. TAYLOR, V. A. JOHNSON, E. A. EMINI, P. DEUTSCH, J. D. LIFSON, S. BONHOEFFER, M. A. NOWAK, AND B. H. HAHN, *Viral dynamics in human immunodeficiency virus type 1 infection*, Nature, 373 (1995), pp. 117–122.
- [66] L. M. WEIN, R. M. D'AMATO, AND A. S. PERELSON, *Mathematical considerations of antiretroviral therapy aimed at HIV-1 eradication or maintenance of low viral loads*, J. Theoret. Biol., 192 (1998), pp. 81–98.
- [67] D. O. WHITE AND F. J. FENNER, *Medical Virology*, Academic Press, New York, 1994.
- [68] S. WOLINSKY, B. T. KORBER, A. U. NEUMANN, M. DANIELS, K. J. KUNSTMAN, A. J. WHETSELL, M. R. FURTADO, Y. CAO, D. D. HO, AND J. T. SAFRIT, *Adaptive evolution of human immunodeficiency virus-type 1 during the natural course of infection*, Science, 272 (1996), pp. 537–542.
- [69] J. K. WONG, M. HEZAREH, H. F. GUNTARD, D. V. HAVLIR, C. C. IGNACIO, C. A. SPINA, AND D. D. RICHMAN, *Recovery of replication-competent HIV despite prolonged suppression of plasma viremia*, Science, 278 (1997), pp. 1291–1295.